NATIONAL UNIVERSITY OF SCIENCE AND TECHNOLOGY
POLITEHNICA BUCHAREST
DOCTORAL SCHOOL OF ELECTRICAL ENGINEERING

SUMMARY
DOCTORAL THESIS

STUDIES ON MULTIPHASE ELECTRIC MOTORS

Scientific coordinator
Professor PhD. Eng. Virgiliu Fireţeanu

Author:
Eng. Constantin Dumitru

BUCHAREST 2023

CONTENTS

INTRODUCTION

The first multiphase motor drive was proposed in 1969, to the knowledge of the author of the thesis, in the paper [1], by PhD. E. E. Ward and Eng. H. Härer, who were working at that time at the University of Southampton, England and University of Stuttgart Institute for Power Transmission and High Voltage Technology, Germany, respectively. In this paper are shown preliminary experiments on a 5-phase induction motor fed by a 10 pulse inverter having thyristors as commutation elements. Compared with a 3-phase induction motor, a threefold reduction in torque ripple was observed. Also, the losses in the motor were high, due to a poor form factor of the line current.

According to the paper [2], from 1969 to 1990, the multiphase motor drives have drawn a limited attention, but from 1990s -2000s, this subject became a focus for the research community, especially for specific application areas, namely electric ship propulsion, electric and hybrid vehicles, high-power industrial applications and electric aircraft.

Paper [3] represents a survey regarding multiphase induction machine (IM) and drive, covering over 30 years of investigation on this subject. This paper analysis three-phase, dual three-phase, five-phase and six-phase IM. A common conclusion of this survey consists on the following advantages of the covered multiphase induction machine over conventional systems:

- Improved reliability, the machine is still operating under specific faulty conditions;
- Reduced iron loss;
- Lower current per phase with the same voltage per phase, useful in applications where there are voltage and current limits, such as electric vehicles;
- Handling of lower power per phase, meaning lower power semiconductors;
- Eliminating certain space harmonics from the air-gap flux, thus eliminating some of the peaks in torque - speed characteristic.

A dynamic numerical model of a multiphase motor with six-phase stator winding and three phase rotor winding is elaborated in the paper [4] and it is shown that the starting transients of current, speed and torque are qualitatively close to that of a three phase induction motor.

In [5] is shown that multiphase electric motors can fulfill the necessary requirements in marine propulsion. It is showed that by increasing the number of phases, the Joule losses in the stator winding can be reduced by several percent, resulting in a higher efficiency. Maintaining the same level of Joule losses, the torque can be increased by a similar percentage, thus the power density can be increased.

In [6], the authors made a comparison of the total harmonic distortion (THD) in the output phase voltage of five phase voltage source inverter. There were considered the following conduction angles: 180°, 162°, 144°, 126° and 108°, of the square waveform, the authors concluded that the lowest THD is obtained for 144°.

More advantages of multiphase machines are described in [2] including:

- The electromagnetic field generated by the stator winding in a multiphase machine has a lower space-harmonic content, thus contributing to the increase of its efficiency;
- It is noted a greater fault tolerance for those types of machines than the three-phase machines, including the ability of self-starting and continuous running but with minimal de-rating;

- Less susceptibility to time-harmonic components of the power system are noticed in those types of machines compared with the three-phase machines. Those components are producing torque pulsations.

Also, in [2] is presented the Clarke's transformation matrix for a symmetrical m-phase system for induction machine with sinusoidal winding distribution connected in star with a single neutral point.

In addition to the general advantages of multiphase machines, among which fault-tolerant capability, reduced torque ripple, higher torque density, an advantage of the multiphase motors is the decrease of around 5% of the stator Joule losses with the increment of the phase number [2] and [7].

The five-phase machine yields 120 possible sequences which can be connected, phase transposition can be calculated from the permutations of the number of phases. Balanced rotating field can be achieved by only 20 connections. Other connections lead to the unbalanced mode, where both first and third sequences are applied to the motor. Ten out of the twenty connections provide full speed because of the first sequence. The other 10 connections run the machine with third of full speed because of the third sequence [8].

Due to limitations in high-power handling, three-phase generators face difficulties in the use of high-power generation in the megawatt range. The use of static VAr (reactive power) compensators implies the following: significant expense, difficult control of the circuit, switching harmonics and transients found in torque ripple implying mechanical vibrations. In this regard, the multiphase machines are utilized in different field of utilizations, for example, EVs (electric vehicles), aircrafts, electric ship propulsion, energy harvesting systems [9], [10], [11] and [12].

Many studies have slowly been redirected to multiphase systems for power generating in independent applications. The examinations in the independent power generation application acquire the benefits of motors as well as permitting ways of using the extra levels of degrees of freedom, for example, the utilization of the interface of power electronic converter in harvesting wind energy systems [10], [13] and [14].

Multiphase machines including five-phase [15], six-phase [16], [17], [18], [19] and [20], seven-phase [13], [21], [22], [23] and twelve-phase [24] have been involved in electrical drives applications in the previous years. Multiphase machines offer advantages that compete with the requirements of the wind industry because they naturally split power up to 10 MW and improve reliability by increasing fault-tolerant capability [10], [15], [22], [23] and [25].

Paper [26] presents a comparison of the induction distribution in different parts, mainly air gap, yoke and teeth of the stator and rotor cores, of an induction motor with five phases between its healthy operation and faulty with two open phases. The analytical model shows very similar results compared to the finite element model and measurements on a prototype. It was found that magnetic flux density in the stator and rotor teeth, in the case of faulty operation, has space harmonics with increased amplitude.

In the papers [27] and [28], the magnetic flux density in the air gap is described through analytical formulas deriving the current sequence components, resulting a time dependence of the magnetic flux density for different speeds. The paper [26] extends the formulations from the above papers in order to include space harmonics of the magnetic flux density, with order higher than the third.

The papers [29] and [30] shows improved performances over a three induction motors with distributed winding compared to the concentrated ones. However, in more recent studies, [31],

[32] and [33], for specific combination of number of phases and slots, is shown that the concentrated windings can offer similar performances compared to distributed winding for healthy and faulty operation. Studies relating the winding type were performed in paper [34] on a six phase induction motor. The pseudo concentrated winding proposed by the authors, with shorter end-winding, shows improved performances over the concentrated winding and worsen performances over the distributed winding.

Some advantages of multiphase (higher than three phases) drives and induction motors are presented in [2], [35], [36], [37], [38] and [39] the tolerance regarding the operation under faulty conditions is one of the main important advantages.

Since the usage of permanent magnets (PM) in the rotors of synchronous machines, the interest in the permanent magnet synchronous motors or generators (PMSM or PMSG) has grown, offering overall better performances in variable speed applications [40], [41], [42], [43], [44], [45], [46] in comparison with the induction machines. Different topologies of PMSMs are analyzed over the time and from the efficiency's point of view, the significantly reduced Joules losses in the rotor and a dedicated electric drive, those types of machines present an important advantage [47], [48], [49], [50], [51], [52] and [53].

This thesis completes and quantifies the fault tolerant argument described in [2], as well as the quantification of the torque ripple. It is observed a diminishing of the electromagnetic torque ripple with the increase of number of stator phases.

In paper [10] are presented three- and seven-phase self-excited induction generators used for a 2.1 [MW] wind turbine model, showing an increase in output power for the seven-phase generator, for the same wind velocity. Also, the paper affirms the capability of the seven-phase generator running under one and two phase failure. The thesis complements the fault tolerance study [10], it is analyzed the capacity of the 7-phase induction motor to operate under certain winding fault conditions, both at start-up and when the fault occurs during operation.

Thesis description

The *general objectives* of the thesis are: the quantitative validation of the information in the literature regarding the behavior and advantages of multiphase machines, the identification of the number of phases, among those studied, which present the best performances for both for the synchronous and induction motors, the design and manufacture of a five-phase induction motor.

This doctoral thesis is structured in five chapters to which are added the introduction and general conclusions, contributions and development perspectives. In the **first chapter** are described the studied cases of induction motors and analyzed the performances for the rated operating point. In the **second chapter** are analyzed the behavior of the 3-phase, 5-phase, 7-phase and 9-phase induction motors, for both steady state tolerance and starting tolerance regarding one or many stator phase's failures. **Chapter three** presents an analysis of multiphase permanent magnet synchronous motors. Those models were developed starting from models of the analogue induction motors, described in the previous chapters. In the **chapter four** are presented formulas and an analysis based on finite element model of five-phase induction motor for healthy operation. Also, an operation point is proposed and analyzed for continuous operation under one open-phase fault considering some criteria. In the **fifth chapter** are presented the manufacturing process the stator laminated stack, the winding process of the stator, the test bench and the results measured on the physical model of the 5-phase squirrel-cage induction motor.

CHAPTER 1. FINITE ELEMENT 2D MODELS OF THE MULTIPHASE (3-5-7-9) SQUIRREL-CAGE INDUCTION MOTORS

In this chapter are described, analyzed and compared the performances of the 3-, 5-, 7- and 9- phase induction motors at rated operation.

1.1. INTRODUCTION

Various studies of squirrel-cage induction machines are carried out on finite element (FE) step by step in time domain models. Coupled field - circuit - rotating motion models are considered, imposing the values corresponding to the supply voltage and of the charge torque.

The magnetic vector potential **A** [0, 0, A (x, y, t)] defines the vector model of the two-dimensional quasi static electromagnetic field in the Cartesian coordinate system, satisfying the equation (1.1). The material properties are the magnetic permeability (μ) and the electric conductivity (σ). The current densities of the stator slots are defined by the vector $\boldsymbol{J_1}$ [0, 0, J_1], respectively, of the squirrel-cage bars, $\boldsymbol{J_2}$, are represented by the term $\sigma \cdot [\partial \mathbf{A}/\partial t]$.

$$curl\left[\left(\frac{1}{\mu}\right)\cdot curl\boldsymbol{A}\right] + \sigma\cdot\left[\frac{\partial A}{\partial t}\right] = \boldsymbol{J_1} \tag{1.1}$$

The electromagnetic field computation's two-dimensional domain, Fig. 1.1, based on the A (x, y, t) potential includes:

- the stator slots – modelled as non-magnetic and non-conductive regions, with $\mu_r = 1$ and $J_1 \neq 0$;
- the rotor slots/bars – regions of solid conductor type, with $\mu_r = 1$ and $J_2 \neq 0$;
- the stator and rotor cores – magnetic nonlinear and nonconductive regions, with $\mu \neq \mu_0$ and $\sigma = 0$;
- electric insulations, air gaps and the neighboring air – non-magnetic and non-conductive regions, with $\mu_r = 1$ and $\sigma = 0$.

Four induction motors (IMs) are analyzed, with different number of phases, namely $m = 3, 5, 7$ and 9. The number of stator slots of each IM are 36, 40, 56 and 36 respectively. The number of rotor slots/bars is the same for the 3-phase, 5-phase and 9-phase motors, namely 28, and the 7-phase motor has 32 bars.

The results presented in this chapter can also be found in the author's paper [55].

In Figure 1.1 is presented the geometry and mesh distribution of the 2D numerical models. An asymptotic space (*Infinite Box*) defines the boundaries of the computation domain. The regions of an induction machine model are described in **Fig. 4.1.** The studies were made using Altair Flux 2D. The skewing effect of the rotor was not considered.

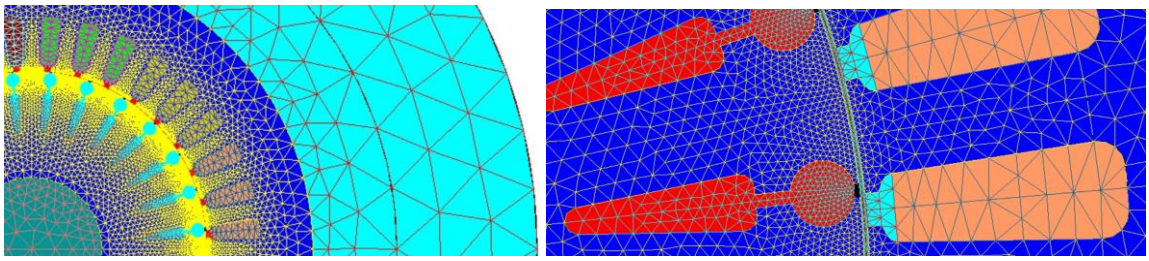

3-phase motor, $Z_1 = 2mpq = 2 \cdot 3 \cdot 2 \cdot 3 = 36$ stator slots

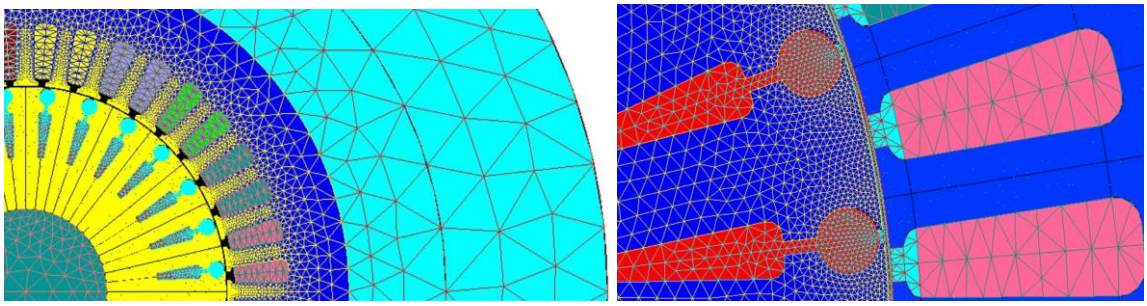

5-phase motor, $Z_1 = 2mpq = 2 \cdot 5 \cdot 2 \cdot 2 = 40$ stator slots

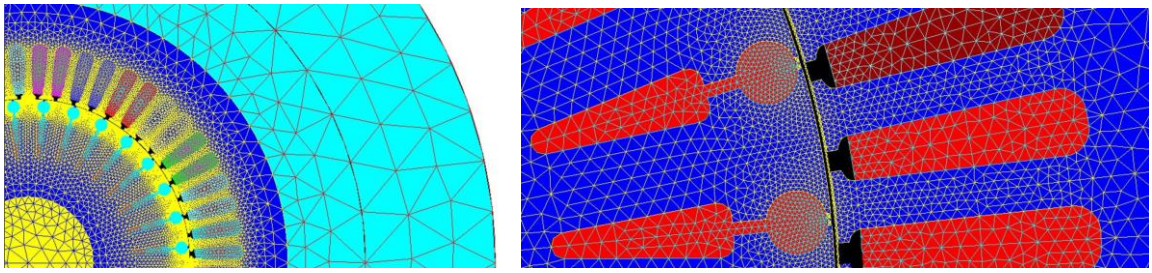

7-phase motor, $Z_1 = 2mpq = 2 \cdot 7 \cdot 2 \cdot 2 = 56$ stator slots

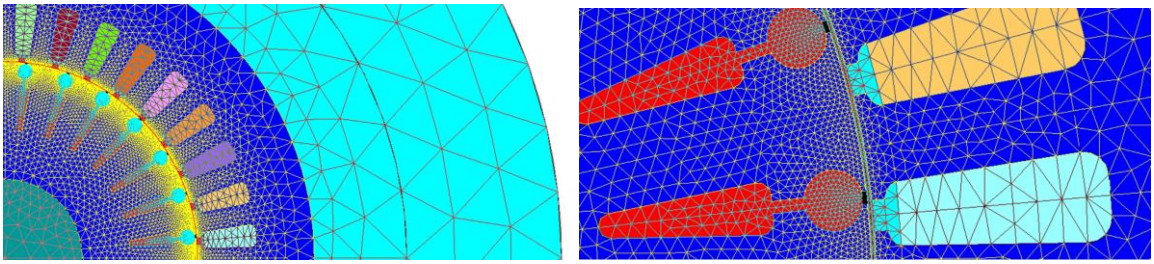

9-phase motor, $Z_1 = 2mpq = 2 \cdot 9 \cdot 2 \cdot 1 = 36$ stator slots

Fig. 1.1. Geometries of the FE models and zoom in the vicinity of the air-gap [55]

Four poles motors with the synchronous speed of 1500 [rpm] and the same main dimensions of the magnetic cores and of the air gap thickness are considered. The electric supply is characterized by the value of the phase to null voltages of 400 [V] and the frequency of 50 [Hz]. The charge operation of the IMs is characterized by the value of the load torque of 50 [Nm] and the moment of inertia of 0.05 [kg·m^2].

The stator winding schemes for the studied multiphase IMs are shown in **Annex 1**, presented in the extended version of the thesis.

1.2. FINITE ELEMENT ANALYSIS OF THE PERFORMANCES OF THE STUDIED IMS

1.2.1. Electromagnetic field results

In this subchapter are analyzed and compared the performances of the motors presented in Fig. 1.1. For all investigated motors, the stator winding has the same number of turns on phase, namely 222. When calculating the phase resistance, the area of the stator slots and the series connection of all the basic coils of the single layer stator winding are taken into account, with a fill factor of 0.55. The phase resistance of the four motors are: 2.247 Ω, 3.369 Ω, 4.396 Ω and 6.738 Ω, respectively. The phase resistances are different because the number of phases, the number of slots per pole and phase, the number of stator slots, the stator slot surface are different from each case. The electric circuits associated with the geometry of the motors are shown in Fig. 1.2.

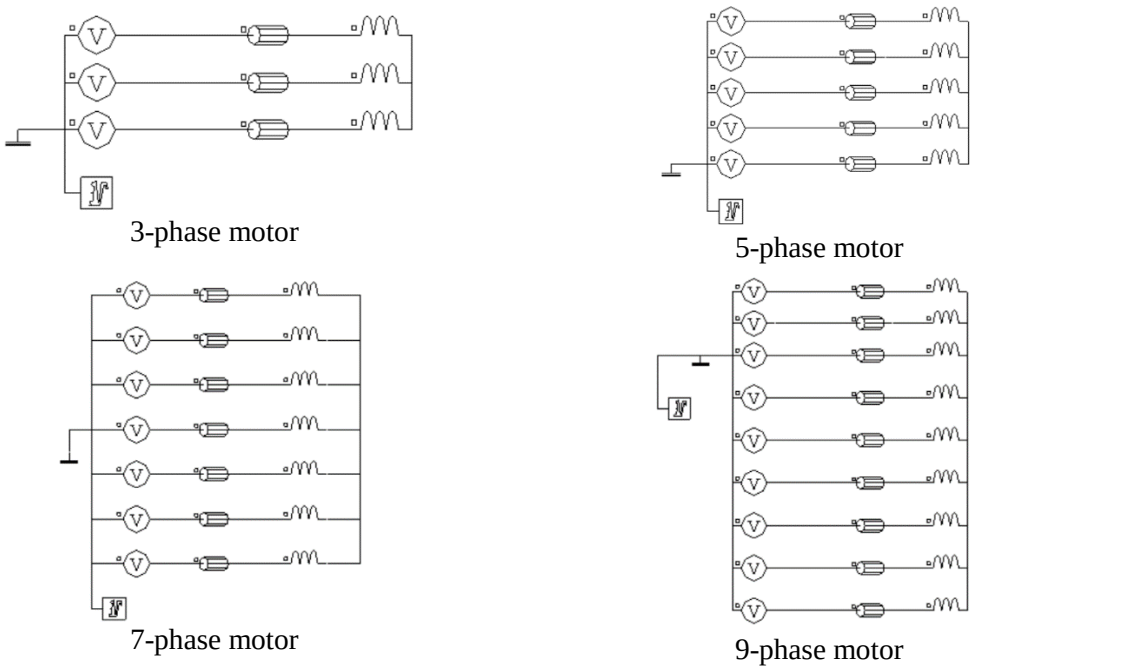

Fig. 1.2. The circuit models of the studied motors [55]

The results below are corresponding to the steady state regime of the electromagnetic field. There were considered a time step value of 0.05 [ms], a coupled load application with the value of resistive torque of 50 [Nm] and with the value of the initial rotor speed of 1450 [rpm] (at t = 0), for a faster transition. The starting current and the starting torque are not evaluated in this type of application.

The maps of the magnetic flux density in the cores of the motors shows a similar magnetic saturation and the quadrupole structure of the electromagnetic field. The maximum values of the magnetic flux density are found in the tips of the stator and rotor teeth. Due to the slotted geometry of the magnetic cores, the content of spatial harmonics of the magnetic flux density is significantly increased. The 7-phase IM presents the lowest content of spatial harmonics of the magnetic flux density, followed by the 9-phase IM.

1.2.2. Stator currents and electromagnetic torque for rated motor's operation and for starting

All the results below are corresponding to the steady state regime of the electromagnetic field. There were considered a time step value of 0.05 [ms] and a coupled load application with the value of load torque of 50 [Nm].

The total content of harmonics of the stator currents, with regard to the 50 [Hz] fundamental of currents, with amplitude above 1 % are: 10.06 %, 14.36 %, 9.36 % and 60.75 %, respectively.

The mean values of the electromagnetic torque of each IM are very similar. The rotor speed is: 1428.4 [rpm], 1426.8 [rpm], 1429.2 [rpm] and 1422.6 [rpm], respectively. The torque ripple is: 24.73 [Nm], 8.857 [Nm], 10.489 [Nm] and 5.943 [Nm], respectively. It was observed that by increasing the number of phases the torque ripple is decreasing. With regard to the mean value of the torque, the total content of the torque harmonics with amplitude above 1 % are: 20.57 %, 6.44 %, 7.41 % and 3.69 %, respectively.

The most important parameter for the characterization of an electrical drive is the efficiency with which electric energy is converted into motion. The following formula was considered for the electric efficiency evaluation:

$$Efficiency\ [\%] = \frac{Mean\ value\ \{Electromagnetic\ Torque\} \cdot Mean\ value\ \{Angular\ Speed\}}{Mean\ value\ \{Active\ Power\ of\ Supply\ Sources\}} \quad (1.2)$$

The outcome results show the 7-phase motor presents the highest efficiency of 91.30 %, followed by the 5-phase motor, with 90.62 %, the 3-phase motor, with 89.86 % and the 9-phase motor with the efficiency of 87.62 %.

1.3. REMARKS

Comparing the steady-state parameters of the studied motors, it is found that (a) the 7 phase motor presents the lowest total harmonic distortion (THD) of normal component of the magnetic flux density along a middle air gap circle, the higher rated speed, the lowest total harmonic distortion of stator currents, the highest electric efficiency and (b) the 9 phase motor presents the lowest ripple of the electromagnetic torque and the lowest total harmonic distortion of the electromagnetic torque.

CHAPTER 2. TOLERANCE REGARDING THE ELECTRIC SUPPLY FAILURES IN THE MULTIPHASE INDUCTION MOTORS

In this chapter are analyzed the behavior of the 3-phase, 5-phase, 7-phase and 9-phase induction machines, the steady state tolerance and the starting tolerance regarding one or many phase failures of the electric supply. The failure of a phase of the electric supply signifies the interruption of that phase and the current through that phase is zero.

An induction machine that before failure operates steady state as induction motor is considered to be **steady state tolerant** with respect a certain failure, if after the failure the new steady state operation it is as induction motor. After the failure the machine continues to operate as induction motor, with operation parameters slightly different from the previous ones.

The **starting tolerance** of an induction machine with respect of phase failures of the electric supply refers to the capability to start and steady state operate as induction motor after starting when one or many phases of the electric supply are interrupted.

The following finite element models are analyzed in the step by step in time domain (TD) and considers the time step value of 0.25 [ms], which is adequate when accounting for the quantities taken into account in the post-processing of the results of the numerical applications.

The results presented in this chapter can also be found in the author's paper [54].

2.1. STEADY STATE TOLERANCE ANALYSIS

In this subchapter are analyzed the steady state tolerance of the 3-phase, 5-phase, 7-phase and 9-phase induction machines.

2.1.1. Steady state tolerance analysis of the 3-phase induction machine

2.1.1.1 Start-up and steady state operation of the healthy 3-phase induction machine

For the 3-phase healthy motor starting in full load of 50 [Nm], the time dependences of the rotor speed and of the electromagnetic torque are shown in Figure 2.1. The circuit associated with the geometry of the 3-phase induction machine with star connected phases and null inaccessible is presented in Figure 2.2.

The steady state operation after starting is characterized by the mean value of the rotor speed of 1429.1 [rpm]. The most important harmonics of the torque are: 5 [Hz] / 0.33 [Nm], 565 [Hz] / 5.35 [Nm], 570 [Hz] / 3.71 [Nm], 865 [Hz] / 1.47 [Nm], 870 [Hz] / 1.09 [Nm].

The RMS values of the stator currents is 7.89 [A]. The amplitudes of the harmonics of the currents are: 50 [Hz] / 11.1 [A], 615 [Hz] / 0.63 [A], 620 [Hz] / 0.40 [A], 815 [Hz] / 0.22 [A].

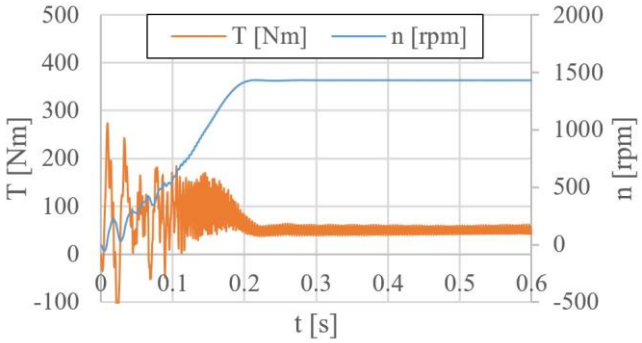

Fig. 2.1. Time dependence of the rotor speed (n) and motor torque (T) during the 3-phase motor starting [54]

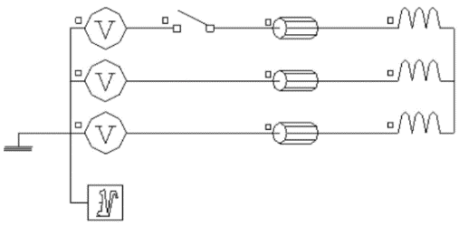

Fig. 2.2. Circuit model of a 3-phase induction machine with star connected phases, null inaccessible and the switch connected to a phase [54]

2.1.1.2 Phase-1 failure after the starting of the 3-phase machine in the healthy state

The failure of a phase of the electric supply is controlled by means of the switch in Fig. 2.2 who change its state (On/Off) at 0.3 [sec], when the steady state of machine operation as motor is achieved.

After the phase failure, the machine operates as generator with the mean value of the rotor speed of -1556 [rpm]. Lowering the value of load torque from 50 [Nm] to 45 [Nm], a similar result is obtained. But, if the load torque decreases at 40 [Nm], the correspondent speed shows that after the Phase-1 failure the machine continues to operate as motor. The new value of the rotor speed is 1398 [rpm]. The new steady state operation of the motor, with the Phase-1 failure, is characterized by the value 120.45 [Nm] of the torque ripple, much higher than the value 22.2 [Nm] in case of healthy motor operation.

Another case of 3-phase machine with star connected phases, null accessible and four conductors electric supply was studied. The new steady state operation of the motor, with the Phase-1 failure, is characterized by the new mean value of the rotor speed of 1408.2 [rpm].

2.1.1.3 Remarks

Comparing the harmonics of the electromagnetic torque between healthy 3-phase IM, Fig. 2.1 and Phase-1 failure of IM with star connected winding and null accessible it is found a shift of harmonic frequencies of the same order, with the amplitudes almost doubled. New harmonics of the electromagnetic torque appear in the faulty case, the most important harmonic is 100 [Hz] / 24.69 [Nm].

The new steady state operation of the motor, with the Phase-1 failure, is characterized by the value 93.56 [Nm] of the torque ripple, higher than the value 22.2 [Nm] in case of healthy motor operation. Regarding the amplitudes of the harmonics of the currents, the phase failure determines an increase up to 62.5% of current for the 50 [Hz] fundamental harmonic.

Since the increase of the harmonics and of the torque ripple is significant, the longtime full-load operation of the 3-phase IM after the Phase-1 failure should be not accepted. Consequently, the 3-phase IM is *not steady state tolerant* to the failure of one phase.

2.1.2. Steady state tolerance analysis of the 5-phase induction machine

2.1.2.1 Start-up and steady state operation of the healthy 5-phase induction machine

The time dependences of the rotor speed and of the electromagnetic torque is shown in Fig. 2.3. In Fig. 2.4 is showed the circuit model of the 5-phase IM associated with its geometry.

For the steady state operation of the 5-phase healthy motor starting in full load of 50 [Nm], the mean value of the rotor speed is 1429.33 [rpm]. The most important harmonics of the torque are: 460 [Hz] / 0.75 [Nm], 465 [Hz] / 0.38 [Nm], 470 [Hz] / 0.40 [Nm], 660 [Hz] / 0.75 [Nm], 770 [Hz] / 0.32 [Nm]. The RMS values of the stator currents is 4.61 [A]. The amplitudes of the harmonics of the currents are: 50 [Hz] / 6.47 [A], 150 [Hz] / 0.13 [A], 615 [Hz] / 0.52 [A], 620 [Hz] / 0.36 [A] and 815 [Hz] / 0.14 [A].

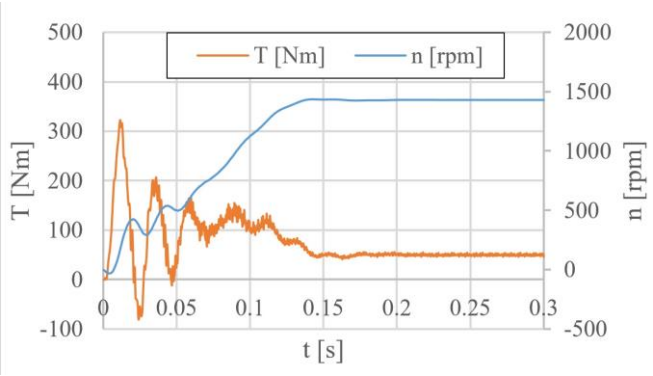

Fig. 2.3. Time dependence of the rotor speed (n) and motor torque (T) during the 5-phase healthy motor starting [54]

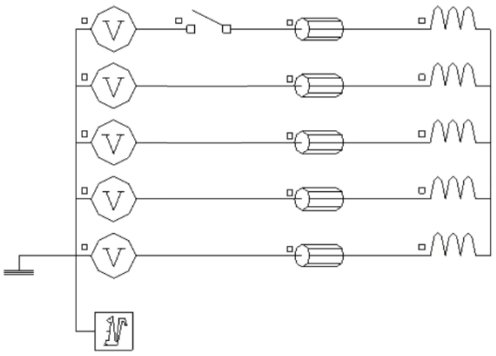

Fig. 2.4. Circuit model of a 5-phase induction machine with star connected phases and the switch connected to a phase

2.1.2.2 Successive failures of stator phases after the start-up of the 5-phase motor in healthy state

The healthy 5-phase induction machine reaches steady-state and at 0.3 [sec] one phase fails. Following a brief transient, the machine continues to function as a motor, Fig. 2.5. The new steady state operation of the motor, with the Phase-1 failure, is characterized by mean value of rotor speed is 1420.68 [rpm], the value 47.52 [Nm] of the torque ripple, much higher than the value 8.2 [Nm] in case of healthy motor operation. The amplitude of the most important harmonic of the electromagnetic torque is 100 [Hz] / 15.73 [Nm]. The RMS values of the stator currents are I_1=0 [A], I_2 = 7.51 [A], I_3 = 4.71 [A], I_4 = 6.2 [A], I_5= 6.86 [A]. The amplitudes of the 50 [Hz] harmonic of the four non-null currents are: 10.56 [A], 6.57 [A], 8.67 [A] and 9.62 [A], respectively.

The 5-phase induction machine starts at full load, at 0.3 [sec] the Phase-1 fails and at 0.45 [sec] the Phase-2 fails. At steady state, the mean value of rotor speed is -543.14 [rpm], thus, the machine operates as electric brake.

If Phase 3 of the 5-phase machine fails at 0.45 [sec] instead of Phase 2, the machine continues to function as a motor and has a steady-state mean rotor speed of 1405.37 [rpm], Fig. 2.6. The value of torque ripple is 76.15 [Nm] in the new steady state motor operation with Phase-1 and Phase-3 failure, significantly higher than the value of 8.2 [Nm] in healthy motor operation. The amplitude of the most important harmonic of the electromagnetic torque is 100 [Hz] / 26.66 [Nm]. The RMS values of the stator currents are I_1=0 [A], I_2=11.03 [A], I_3=0 [A], I_4=9.5 [A] and I_5=7.4 [A]. The amplitudes of the 50 [Hz] harmonic of the three non-null currents are: 15.50 [A], 13.22 [A] and 10.32 [A], respectively.

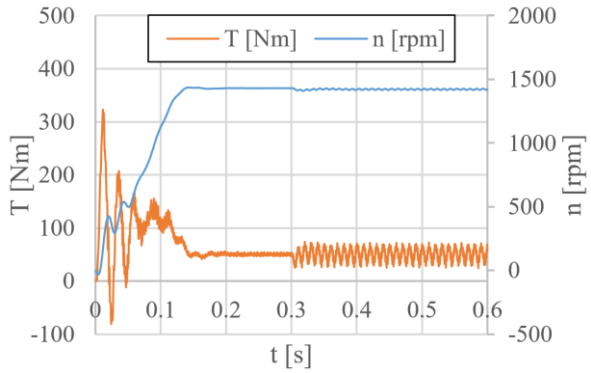

Fig. 2.5. Phase-1 failure after the full load stating of the healthy 5-phase machine [54]

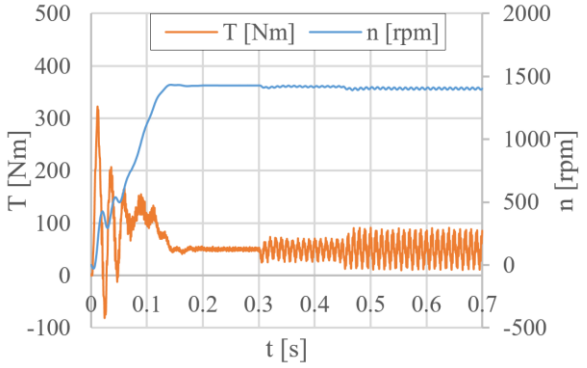

Fig. 2.6. Successive failures Phase-1 and Phase-3 after the full load starting of the healthy 5-phase machine [54]

Phase-1 fails at 0.3 seconds, Phase-2 fails at 0.4 [sec], and Phase-3 fails at 0.5 [sec] following the full load start of the 5-phase induction machine. Another case is evaluated where Phase-4 fails at 0.5 [sec], instead the Phase-3. At the end of transients, the mean value of rotor speed is -1717.2 [rpm] in the first case and -1567.04 [rpm] in the second case, thus the machine operates as asynchronous generator. As a result, the 5-phase motor is not steady state tolerant regarding the failure of three phases of the electric supply.

2.1.2.3 Remarks

The decrease of the supply currents, of the amplitudes of the torque and current harmonics and of the torque ripple from 22.2 [Nm] to 8.2 [Nm], in case of the 5-phase motor compared with the 3-phase motor are important advantages.

Comparing the cases (a) healthy 5-phase IM, Fig. 2.3, (b) Phase-1 failure, Fig. 2.5 and (c) Phase-1 and Phase-3 failures, Fig. 2.6, it is found that:

- the increase of the slip of steady state operation from 4.7% to 5.3% and to 6.3%, respectively the decrease of the rotor speed generated by the failures should be acceptable for the continuation for a time of the operation of the 5-phase motor after the correspondent failures;
- the important increase of torque ripple from 8.2 [Nm] to 47.52 [Nm] and to 76.15 [Nm], respectively, should be unacceptable for the longtime continuation of the 5-phase motor operation after failures;
- the appearance of a new torque harmonic of 100 [Hz] is noted in the cases (b) and (c), with the amplitudes of 15.73 [Nm] and 26.66 [Nm], respectively;
- the fundamental harmonic (50 [Hz]) of the currents increases roughly 1.6 times (b) and 2.4 times (c) compared to the healthy 5-phase IM case (a).

Consequently, the 5-phase induction motor should be considered tolerant to the failure of two phases of the electric supply, if these phases are not adjacent.

2.1.3. Steady state tolerance analysis of the 7-phase induction machine

2.1.3.1 Starting and steady state operation of the healthy 7-phase machine

The healthy 7-phase motor starts at full load of 50 [Nm] and in steady state operation reaches the mean rotor speed of 1428.3 [rpm], Fig. 2.7. In Fig. 2.8 is showed the circuit model of the 7-phase IM. The most important harmonics of the torque are: 10 [Hz] / 0.165 [Nm], 105 [Hz] / 0.163 [Nm], 655 [Hz] / 0.535 [Nm], 660 [Hz] / 1.917, 665 [Hz] / 1.049 [Nm], 670 [Hz] / 0.363 [Nm], 1215 [Hz] / 0.198 [Nm], 1225 [Hz] / 0.587 [Nm] and 1230 [Hz] / 0.457 [Nm]. The RMS values of the seven stator currents is 2.81 [A]. The amplitudes of the harmonics of the currents are: 50 [Hz] / 3.963 [A], 710 [Hz] / 0.085 [A], 810 [Hz] / 0.083 [A], 1085 [Hz] / 0.082 [A].

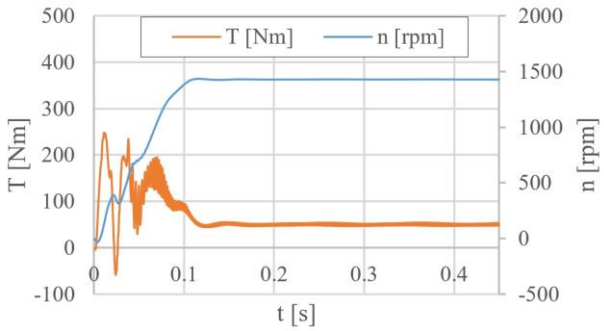

Fig. 2.7. Time dependence of the rotor speed (n) and motor torque (T) during the 7-phase healthy motor starting [54]

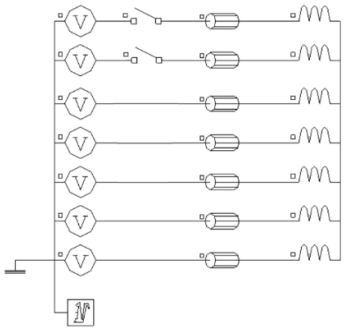

Fig. 2.8. Circuit model of a 7-phase induction machine with star connected phases

2.1.3.2 Successive failures of stator phases after the starting of the 7-phase machine in healthy state

For this study, the 7-phase machine starts with full load, Phase-1 fails at 0.15 [sec] and Phase-2 fails at 0.3 [sec], Fig. 2.9, the switches in Fig. 2.8 changes state. The induction machine continues to operate as motor, even though two adjacent phases fail successively. In the steady state operation, the motor with the Phase-1 failure has the mean value of rotor speed is 1425.3 [rpm] and the electromagnetic torque ripple is 26.31 [Nm]. In the case of Phase-1 and Phase-2 failures, the motor reaches the mean value of rotor speed 1414.94 [rpm] and the value 47.81 [Nm] of the torque ripple, much higher than the value 6.54 [Nm] in case of healthy motor operation. The amplitude of the most important harmonic of the electromagnetic torque is 100 [Hz] / 18.65 [Nm]. The RMS values of the stator currents are I_1=0 [A], I_2=0 [A], I_3=5.7 [A], I_4=3.66 [A], I_5=3.75 [A], I_6=4.16 [A] and I_7=5.53 [A]. The amplitude of the 50 [Hz] harmonic of the five non-null currents are: 8.03 [A], 5.16 [A], 5.28 [A], 5.87 [A] and 7.81 [A].

After three successive failures, the Phase-1 fails at 0.25 [sec], the Phase-2 fails at 0.4 [sec] and the Phase-3 fails at 0.55 [sec], the 7-phase machine does not change its motor operation behavior. The new steady state operation of the motor, with the three phases failures, is characterized by the mean value of speed 1351.1 [rpm] and the value 87.8 [Nm] of the torque ripple. The amplitude of the most important harmonic of the electromagnetic torque is 100 [Hz] / 33.15 [Nm]. The RMS values of currents are I_1=0 [A], I_2=0 [A], I_3=0 [A], I_4=11.15 [A], I_5=6.02 [A], I_6=6 [A] and I_7=10.59 [A]. The amplitude of the 50 [Hz] harmonic of the four non-null currents are: 15.73 [A], 8.48 [A], 8.43 [A], and 14.94 [A].

After three successive failures, the Phase-1 fails at 0.25 [sec], the Phase-3 fails at 0.4 [sec] and the Phase-5 fails at 0.55 [sec], Fig. 2.10, the 7-phase machine does not change its motor operation behavior. The new steady state operation of the motor, with the three phases failures,

is characterized by the mean value of speed 1409.96 [rpm] and the value 36.4 [Nm] of the torque ripple, lower than the similar case of three phases failure. The amplitude of the most important harmonic of the electromagnetic torque is 100 [Hz] / 8.62 [Nm]. The RMS values of currents are I_1=0 [A], I_2=6.26 [A], I_3=0 [A], I_4=6.33 [A], I_5=0 [A], I_6=4.88 [A] and I_7=4.73 [A]. The amplitude of the 50 [Hz] harmonic of the four non-null currents are: 8.81 [A], 8.90 [A], 6.87 [A], and 6.65 [A].

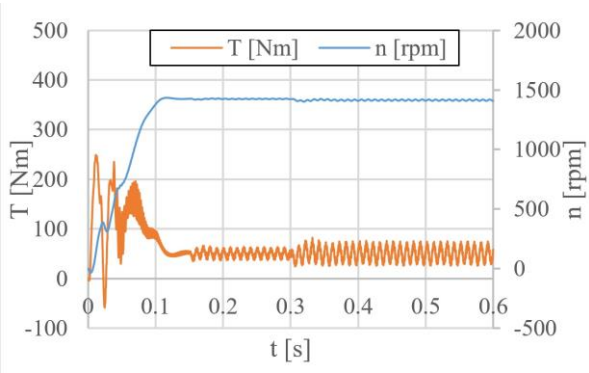

Fig. 2.9. Phase-1 and Phase-2 failures after the full load stating of the healthy 7-phase motor [54]

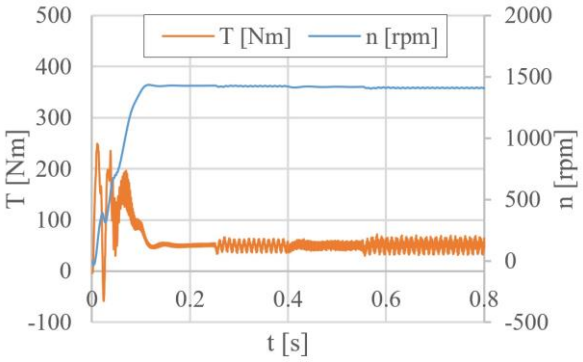

Fig. 2.10. Successive failures of the Phases -1, -3 and -5 after the full load starting of the healthy 7-phase machine [54]

After three successive failures, the Phase-1 fails at 0.25 [sec], the Phase-4 fails at 0.4 [sec] and the Phase-7 fails at 0.55 [sec], the 7-phase machine does not change its motor operation behavior. The new steady state operation of the motor, with the three phases failures, is characterized by the mean value of speed 1404.7 [rpm] and the value 73.73 [Nm] of the torque ripple. The amplitude of the most important harmonic of the electromagnetic torque is 100 [Hz] / 30.27 [Nm]. The RMS values of currents are I_1=0 [A], I_2=6.48 [A], I_3=5 [A], I_4=0 [A], I_5=5.84 [A], I_6=6.1 [A] and I_7=0 [A]. The amplitude of the 50 [Hz] harmonic of the four non-null currents are: 9.10 [A], 7.03 [A], 8.21 [A], and 8.58 [A].

For this study, the 7-phase machine starts with full load and is followed by four successive failures: Phase-1 fails at 0.25 [sec], Phase-2 fails at 0.4 [sec], Phase-3 fails at 0.55 [sec] and Phase-4 fails at 0.7 [sec]. The 7-phase machine, after four successive failures, operates steady-state as an electric generator.

However, the 7-phase machine continues to function as a motor if the four successive failures are applied to the Phase-1, -3, -5 and -7. The mean value of the rotor speed is 1381.58 [rpm] and the value of the torque ripple is 52.96 [Nm]. The amplitude of the most important harmonic of the electromagnetic torque is 100 [Hz] / 13.67 [Nm]. The RMS values of currents are I_1=0 [A], I_2=9.1 [A], I_3=0 [A], I_4=7.8 [A], I_5=0 [A], I_6=9.25 [A] and I_7=0 [A]. The amplitude of the 50 [Hz] harmonic of the three non-null currents are: 12.82 [A], 10.98 [A] and 13.05 [A].

2.1.3.3 Remarks

The decrease of the supply currents, of the amplitudes of the torque and current harmonics, also, of the torque ripple from 8.2 [Nm] to 6.54 [Nm], in case of the 7-phase motor in healthy operation compared with the healthy 5-phase motor, are important advantages.

In subchapter 2.1.3 is shown that the case of interrupting Phase-1, Phase-3 and Phase-5 (non-adjacent phases) has the lowest impact of functional parameters, so this case remains representative for three phases failures of the 7-phase IM.

Comparing the cases (a) healthy 7-phase IM, Fig. 2.7, (b) failure of Phase-1 and Phase-2, Fig. 2.9, (c) failure of Phase-1, -3 and -5, Fig. 2.10, and (d) failure of Phase-1, -3, -5 and -7, it is found that:

- the increase of the slip of steady state operation from 4.78% to 5.67%, to 6% and to 7.9%, respectively the decrease of the rotor speed generated by the failures should be acceptable for the continuation for a time of the operation of the 7-phase motor after the correspondent failures;
- the increases of torque ripple from 6.54 [Nm] to 47.8 [Nm], to 36.4 [Nm] and to 52.96 [Nm], respectively, should be unacceptable for the longtime continuation of the 7-phase motor operation after failures;
- the appearance of a new torque harmonic of 100 [Hz] is noted in the cases (b), (c) and (d), with the amplitudes of 18.65 [Nm], 8.62 [Nm] and 13.67 [Nm], respectively;
- the fundamental harmonics (50 [Hz]) of the currents increases roughly 2 times (b), 2.2 times (c) and 3.3 (d) compared to the healthy 7-phase IM case (a).

Consequently, the 7-phase induction motor should be considered tolerant to the failure of two phases and three non-adjacent phases of the electric supply.

2.1.4. Steady state tolerance analysis of the 9-phase induction machine

2.1.4.1 Starting and steady state operation of the healthy 9-phase machine

In the case of the 9-phase healthy motor starting in full load of 50 [Nm], the time dependences of the rotor speed and of the electromagnetic torque are shown in Fig. 2.11. In Fig. 2.12 is showed the circuit model of the 9-phase IM. The mean value of the rotor speed is 1428.57 [rpm]. The most important harmonics of the torque are: 260 [Hz] / 0.22 [Nm], 565 [Hz] / 0.78 [Nm], 570 [Hz] / 0.34 [Nm], 575 [Hz] / 0.24 [Nm], 865 [Hz] / 1.22 [Nm], 875 [Hz] / 0.26 [Nm]. The mean RMS values of the stator currents is 2.7 [A]. The amplitudes of the harmonics of the currents are: 50 [Hz] / 3.56 [A], 515 [Hz] / 0.12 [A], 615 [Hz] / 0.64 [A], 620 [Hz] / 0.34 [A], 715 [Hz] / 0.73 [A], 720 [Hz] / 0.35 [A].

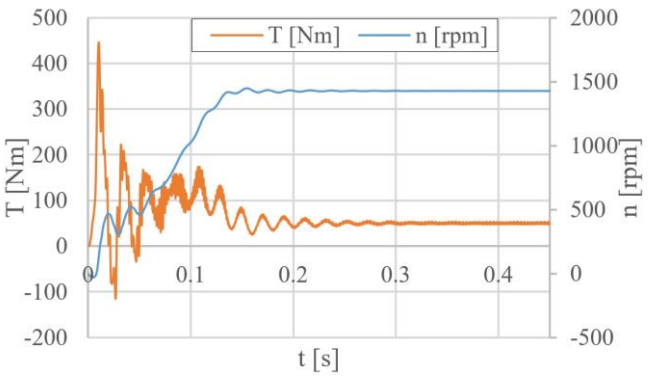

Fig. 2.11. Time dependence of the rotor speed (n) and motor torque (T) during the 9-phase healthy motor starting [54]

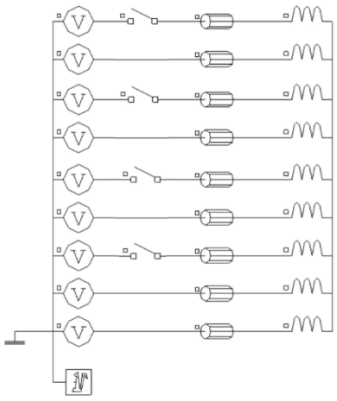

Fig. 2.12. Circuit model of a 9-phase induction machine with star connected phases

2.1.4.2 Successive failures of stator phases after the starting of the 9-phase motor in healthy state

For this study, the 9-phase machine starts with full load and is followed by four successive failures: Phase-1 fails at 0.3 [sec], Phase-3 fails at 0.4 [sec], Phase-5 fails at 0.5 [sec] and Phase-7 fails at 0.6 [sec], Fig. 2.13. The 9-phase machine, after four successive failures,

continues to function as a motor. The mean value of the rotor speed is 1407.7 [rpm] and the torque ripple is 86 [Nm], much higher than the value 6.37 [Nm] in case of healthy motor operation. The amplitude of the most important harmonic of the electromagnetic torque is 100 [Hz] / 4.69 [Nm]. The RMS values of the stator currents are I_1=0 [A], I_2=5.83 [A], I_3=0 [A], I_4=5.88 [A], I_5=0 [A], I_6=6.06 [A], I_7=0 [A], I_8=5.89 [A] and I_9=4.52 [A]. The amplitude of the 50 [Hz] harmonic of the five non-null currents are: 7.97 [A], 7.98 [A], 8.27 [A], 7.52 [A] and 6.02 [A].

At the times of 0.3, 0.4, 0.5, 0.6 and 0.8 [sec], corresponding to the Phase-1, -3, -5, -7 and -9, following the healthy 9-phase machine's full load start, this machine continues to operate as a motor, Fig. 2.14. The mean value of rotor speed is 1377.5 [rpm] and the electromagnetic torque ripple is 157.5 [Nm]. The amplitude of the most important harmonic of the electromagnetic torque is 100 [Hz] / 11.27 [Nm]. The RMS values of the stator currents are I_1=0 [A], I_2=9.15 [A], I_3=0 [A], I_4=6.86 [A], I_5=0 [A], I_6=8.16 [A], I_7=0 [A], I_8=8.86 [A] and I_9=0 [A]. The amplitude of the 50 [Hz] harmonic of the four non-null currents are: 12.62 [A], 9.26 [A], 11.07 [A], and 12.15 [A].

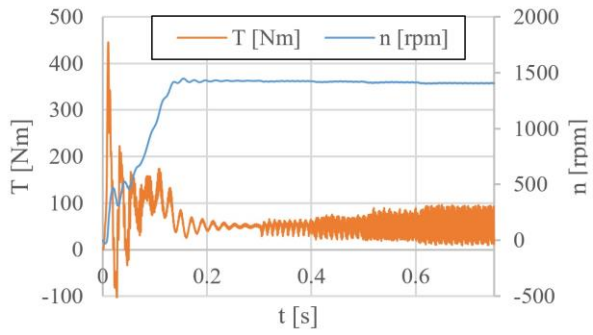

Fig. 2.13. Successive failures of the Phase-1, -3, -5 and -7 after the full load starting of the healthy 9-phase machine [54]

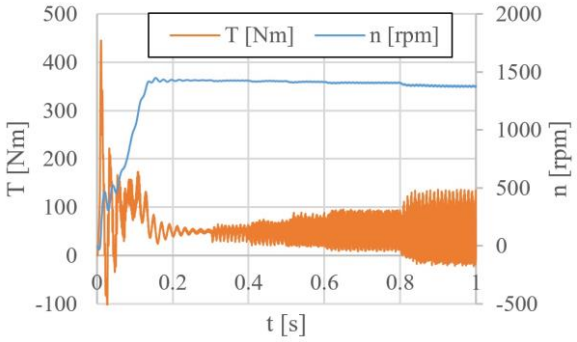

Fig. 2.14. Successive failures of the Phase-1, -3, -5, -7 and -9 after the full load starting of the healthy 9-phase machine [54]

2.1.4.3 Remarks

The decrease of the supply currents, of the amplitudes of the torque and current harmonics and the torque ripple from 22.2 [Nm] to 6.37 [Nm], in case of the 9-phase motor compared with the 3-phase motor are important advantages.

Comparing the cases (a) healthy 9-phase IM, Fig. 2.11, (b) four phases failure, Fig. 2.13 and (c) five phases failure, Fig. 2.14, it is found that:

- the increase of the slip of steady state operation from 4.76% to 6.16% and to 8.17%, respectively the decrease of the rotor speed generated by the failures should be acceptable for the continuation for a time of the operation of the 9-phase motor after the correspondent failures;
- the very important increase of torque ripple from 6.37 [Nm] to 86 [Nm] and to 157.5 [Nm], respectively, should be unacceptable for the longtime continuation of the 9-phase motor operation after failures;
- the appearance of a new torque harmonic of 100 [Hz] is noted in the cases (b) and (c), with the amplitudes of 25.86 [Nm], 38.95 [Nm], respectively;
- the fundamental harmonic (50 [Hz]) of the currents increases roughly 2.3 times (b) and 3.5 times (c) compared to the healthy 9-phase IM case (a).

Consequently, the 9-phase induction motor should be considered tolerant to the failure of four non-adjacent phases of the electric supply.

2.2. STARTING TOLERANCE ANALYSIS

In this subchapter is analyzed the starting tolerance of the 3-phase, 5-phase, 7-phase and 9-phase induction machines.

2.2.1. Starting tolerance analysis of 3-phase IM with the Phase-1 failure

Considering the reduced load of 5 [Nm], the Phase-1 interrupted (switch Off in Fig. 2.2) and the inaccessibility of the star connection of the stator winding, it is found that the machine operates steady state as electric brake. The mean value of the rotor speed is -110 [rpm] and it presents very important oscillations. In the presence of four conductors supply, the Phase-1 failure and the reduced load torque of 30 [Nm], the start-up tentative of the 3-phase machine is characterized by the rotor speed of 488.6 [rpm] and important oscillations of the electromagnetic torque. Therefore, the 3-phase induction machine cannot operate as a motor with one phase failure, with star connected stator winding, even with four conductors electric supply (null accessible).

2.2.2. Starting tolerance analysis of 5-phase IM with one phase and two phases failures

In Fig. 2.15 is represented the starting of the 5-phase motor, with the Phase-1 failure and the mean value of the rotor speed is 1420.63 [rpm]. The amplitude of the most important harmonic of the electromagnetic torque is 100 [Hz] / 15.71 [Nm]. The RMS values of currents are I_1=0 [A], I_2=7.52 [A], I_3=4.7 [A], I_4=6.17 [A] and I_5=6.86 [A]. The amplitude of the 50 [Hz] harmonic of the four non-null currents are: 10.57 [A], 6.58 [A], 8.68 [A] and 9.63[A].

In Fig. 2.16 is shown the starting of the same motor but with Phase-1 and Phase-3 failures, the mean value of the speed is 478.3 [rpm] and non-negligible oscillations.

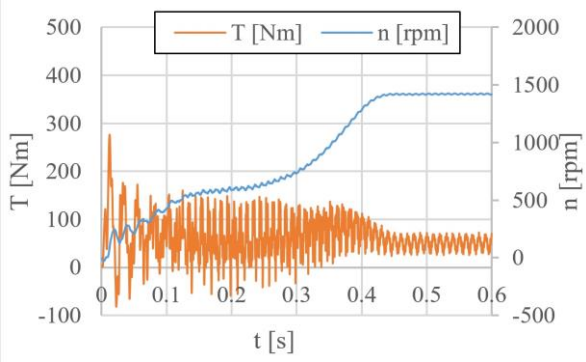

Fig. 2.15. Starting of the 5-phase motor with hase-1 failure [54]

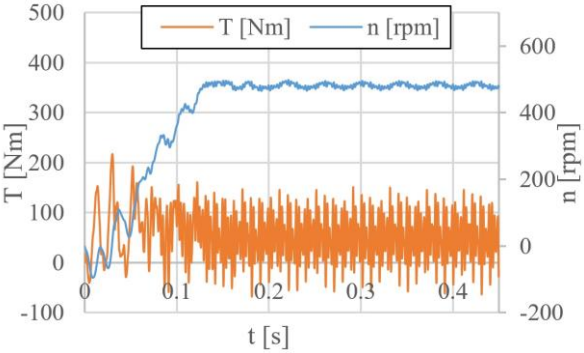

Fig. 2.16. Starting of the 5-phase motor with Phase-1 and Phase-3 failures [54]

Remarks

Comparing the cases (a) healthy 5-phase IM, Fig. 2.3 and (b) starting of the 5-phase motor with Phase-1 failure, Fig. 2.15, it is found that:

- the increase of the slip of steady state operation from 4.7% to 5.3%, respectively the decrease of the rotor speed generated by the failures should be acceptable for the continuation for a time of the operation of the 5-phase motor after the correspondent failures;
- the important increase of torque ripple from 8.2 [Nm] to 47 [Nm] should be unacceptable for the longtime continuation of the 5-phase motor operation after failures;
- the appearance of a new torque harmonic of 100 [Hz] is noted in the case (b), with the amplitudes of 15.71 [Nm];

- the fundamental harmonic (50 [Hz]) of the currents increases roughly 1.6 times (b) compared to the healthy 5-phase IM case (a).

The 5-phase induction motor can be considered starting tolerant only with one phase failure.

2.2.3. Starting tolerance analysis of 7-phase IM with one phase and two phases failures

The steady state mean value of the rotor speed is 1425.1 [rpm], for the 7-phase IM started with Phase-1 failure, Fig. 2.17. The amplitude of the most important harmonic of the electromagnetic torque is 100 [Hz] / 7.93 [Nm]. The RMS values of currents are I_1=0 [A], I_2=3.6 [A], I_3=3.15 [A], I_4=2.97 [A], I_5=3.21 [A], I_6=3.28 [A] and I_7=3.73 [A]. The amplitude of the 50 [Hz] harmonic of the six non-null currents are: 5.58 [A], 4.44 [A], 4.19 [A], 4.53 [A], 4.62 [A] and 5.27 [A].

The steady state mean value of the rotor speed is 1418.6 [rpm], for the 7-phase IM started with Phase-1 and Phase-3 failures, Fig. 2.18. The amplitude of the most important harmonic of the electromagnetic torque is 100 [Hz] / 0.49 [Nm]. The RMS values of currents are I_1=0 [A], I_2=5.6 [A], I_3=0 [A], I_4=4.5 [A], I_5=3.64 [A], I_6=3.4 [A] and I_7=4.3 [A]. The amplitude of the 50 [Hz] harmonic of the five non-null currents are: 7.89 [A], 6.30 [A], 5.14 [A], 4.77 [A], and 6.07 [A].

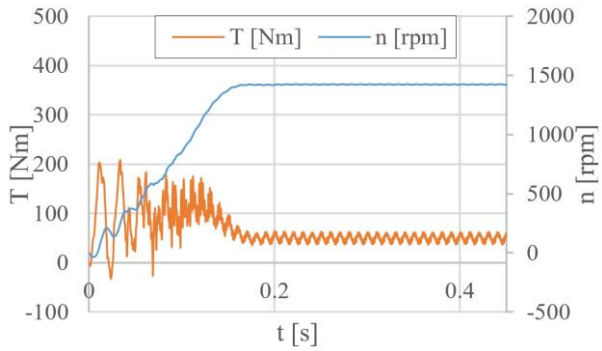

Fig. 2.17. Starting of the 7-phase motor with Phase-1 failure [54]

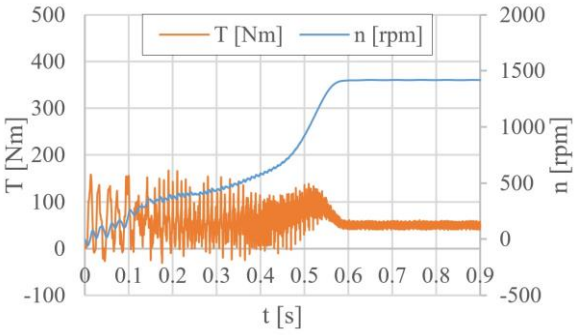

Fig. 2.18. Starting of the 7-phase motor with Phase-1 and Phase-3 failures [54]

Similar studies have been conducted on the 7-phase induction motor starting. It is noted that for the phase pairs:

- Phase-1 and Phase -2 failures, the machine operates steady state as an electric brake with the mean value of speed-285 [rpm], and important oscillations of the rotor speed and torque;
- for both pairs: Phase-1, -4; Phase-1, -5, the motor is characterized by a mean value slightly over 500 [rpm] and important oscillations of the rotor speed and torque.

Three studies have been conducted on the 7-phase induction motor starting with respect the failure of 3 or 4 phases, the results showed that the machine operates steady state as an electric brake or generator. The cases considered are:

- Failure of Phase-1, -3 and -5, with the mean value of speed is -481.3 [rpm];
- Failure of Phase-1, -2, -3 and -4, with the mean value of speed is -1568.8 [rpm];
- Failure of Phase-1, -3, -5 and -7, with the mean value of speed is -500 [rpm].

Remarks

Comparing the cases (a) healthy 7-phase IM, Fig. 2.7, (b) starting of the 7-phase motor with Phase-1 failure, Fig. 2.17 and (c) starting of the 7-phase motor with Phase-1 and Phase-3 failures, Fig. 2.18, it is found that:

- the increase of the slip of steady state operation from 4.7% to 5% and to 5.4%, respectively the decrease of the rotor speed generated by the failures should be acceptable for the continuation for a time of the operation of the 7-phase motor after the correspondent failures;
- the increase of torque ripple from 6.54 [Nm] to 25.8 [Nm] and to 18.12 [Nm], respectively, should be unacceptable for the longtime continuation of the 7-phase motor operation after failures;
- the appearance of a new torque harmonic of 100 [Hz] is noted in the case (b), with the amplitudes of 7.93 [Nm];
- the fundamental harmonic (50 [Hz]) of the currents increases roughly 1.4 times (b) and 2 times (c) compared to the healthy 7-phase IM case (a).

The 7-phase motor is considered to be starting tolerant for its operation under one phase failure and under two non-adjacent phases failure.

2.2.4. Starting tolerance analysis of 9-phase IM with up to three phase failures

The steady state mean value of the rotor speed is 1425.8 [rpm], for the 9-phase IM started with Phase-1 failure, Fig. 2.19. The amplitude of the most important harmonic of the electromagnetic torque is 100 [Hz] / 5.92 [Nm]. The RMS values of currents are I_1=0 [A], I_2=3.7 [A], I_3=3.18 [A], I_4=2.8 [A], I_5=2.76 [A], I_6=3.25 [A], I_7=2.9 [A], I_8=3.12 [A] and I_9=3.28 [A]. The amplitude of the 50 [Hz] harmonic of the non-null currents are: 4.93 [A], 4.19 [A], 3.68 [A], 3.66 [A], 4.31 [A], 3.83 [A], 4.13 [A] and 4.40 [A].

The steady state mean value of the rotor speed is 1420.4 [rpm], for the 9-phase IM started with Phase-1 and Phase-2 out of work, Fig. 2.20. The amplitude of the most important harmonic of the electromagnetic torque is 100 [Hz] / 13.47 [Nm]. The RMS values of currents are I_1=0 [A], I_2=0 [A], I_3=4.93 [A], I_4=3.67 [A], I_5=2.87 [A], I_6=3.47 [A], I_7=3.81 [A], I_8=3.67 [A] and I_9=4.2 [A]. The amplitude of the 50 [Hz] harmonic of the non-null currents are: 6.64 [A], 4.78 [A], 3.77 [A], 4.64 [A], 5.02 [A], 4.84 [A] and 5.66 [A].

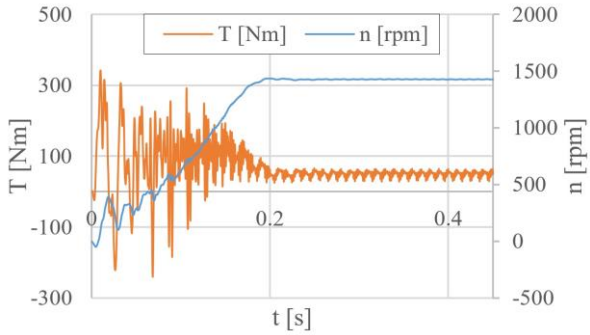

Fig. 2.19. Starting of the 9-phase motor with Phase-1 failure [54]

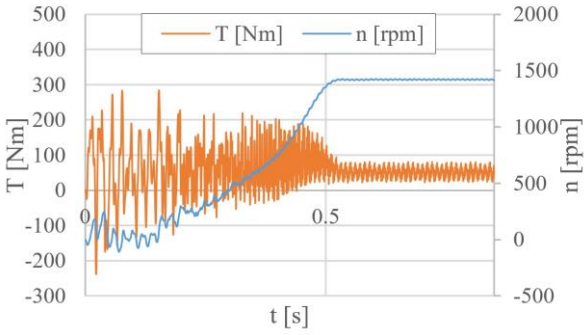

Fig. 2.20. Full load starting of the 9-phase motor with Phase-1 and Phase-2 failure [54]

Comparing all cases of two-phase failures of 9-phase IM, the highest values of amplitudes of harmonics and the torque ripple are presented above, in case of failure of Phase-1 and Phase-2, the difference compared to others is less than 10%.

The steady state mean value of the rotor speed is slightly over 320 [rpm] with important oscillations, for the 9-phase IM started with Phase-1, -4 and -7 out of work. Therefore, the fault tolerance related the 9-phase motor starting is not characterized by the three phase failures.

Remarks

Comparing the cases (a) healthy 9-phase IM, Fig. 2.11, (b) starting of the 9-phase motor with Phase-1 failure, Fig. 2.19 and (c) starting of the 9-phase motor with Phase-1 and Phase-2 failures, Fig. 2.20, it is found that:

- the increase of the slip of steady state operation from 4.76% to 4.95% and to 5.3%, respectively the decrease of the rotor speed generated by the failures should be acceptable for the continuation for a time of the operation of the 9-phase motor after the correspondent failures;
- the important increase of torque ripple from 6.37 [Nm] to 36.34 [Nm] and to 57.74 [Nm], for case (c) should be unacceptable for the longtime continuation of the 9-phase motor operation after failures;
- the appearance of a new torque harmonic of 100 [Hz] is noted in the cases (b) and (c), with the amplitudes of 5.92 [Nm] and 13.47 [Nm], respectively;
- the fundamental harmonic (50 [Hz]) of the currents increases roughly 1.4 times (b) and 1.9 times (c) compared to the healthy 9-phase IM case (a).

The 9-phase motor is considered to be starting tolerant for its operation under one phase failure and under two phases failure.

2.3. REMARKS

Two type of the tolerance regarding the electric supply faults have been studied - the steady state tolerance, associated with the steady state full charge motor operation and the starting tolerance associated with the full charge motor starting. The IM is considered to be tolerant if the values of functional parameters at the final steady state are close to those in healthy operation.

The three-phase IM should be considered (1) not steady state tolerant regarding the failure of one phase due to increase of the torque and currents harmonics and important torque ripple, therefore the longtime full-load operation should be not accepted. Also, the three-phase IM should not be considered (2) starting tolerant in case of one phase failure even with star connected phases, null accessible and four conductors electric supply.

The five-phase induction motor should be considered (1) steady state tolerant regarding the failures of one phase and two non-adjacent phases and (2) starting tolerant only with one phase failure.

The seven-phase IM should be considered (1) steady state tolerant to the failures of one phase, two phases, three phases. The starting tolerance (2) can be associated to the motor in cases of the failure of one phase and even of the failures of two specific phases, such as Phase-1, -3; Phase-2, -4; Phase-3, -5 etc.

The nine-phase induction motor should be considered (1) steady state tolerant regarding the failures of one phase, two phases, three phases and four non-adjacent phases. The starting tolerance (2) can be associated to the motor in case of the failure of one phase and even of the failures of two phases.

For studied cases, the seven-phase induction motor presents the best behavior regarding the failure of phases of the electric supply.

CHAPTER 3. RESEARCHES ON PERMANENT MAGNET SYNCHRONOUS MULTIPHASE MOTORS

In this chapter is presented an analysis based on finite element (FE) models of multiphase permanent magnet synchronous motors (PMSM). Those models were developed starting from models of the analogue induction motors (IM), presented in the previous chapters. The investigation of the PMSMs in this chapter is based on magneto-static and on step by step in time domain FE models. Some results presented in this chapter can also be found in the author's paper [56].

3.1. FINITE ELEMENT 2D MODELS OF THE MULTIPHASE PERMANENT MAGNET SYNCHRONOUS MOTORS

The stator winding configurations, the stator geometry and meshing are identical to those of the analogue induction motors, with same general parameters. The imposed rated rotor speed of 1500 [rpm], or the synchronous speed, characterizes all four PMS motors. The electric supply is taken into account as a current source in the PMSM's circuit models, which will be discussed further in subchapter 3.3 and Fig. 3.3.

The squirrel-cage rotors of IMs are replaced by a simple rotor configuration with four interior permanent magnets (PM) characterized by the remnant magnetic flux density of 1.2 [T] and relative magnetic permeability of 1.05, the geometry of the rotor is presented in Fig. 3.1. The rated load torque is 50 [Nm], the moment of inertia is 0.05 [kg·m^2].

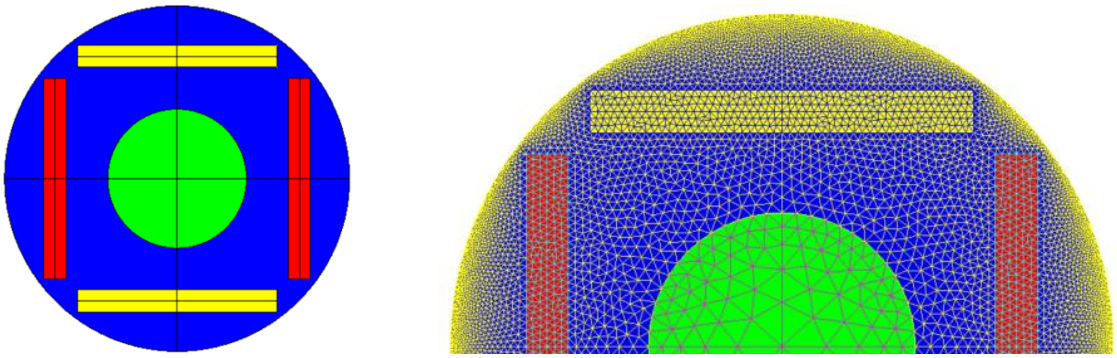

Fig. 3.1. Geometry and mesh distribution of the rotor of PMS motors [56]

For cogging torque evaluation are considered magneto-static rotor multi-position models with an angular step value of 0.2 [degrees]. For all time dependent analyses are considered the finite element in time domain models, considering coupled field - circuit - rotating motion models, with a time step value of 50 [μs]. The results corresponding to the steady state regime of the electromagnetic field are analyzed.

The geometrical dimensions of the magnets are imported from a standard Flux model, those weren't optimized in order to obtain a sinusoidal wave of the magnetic flux density, even if those motor are fed from a sinusoidal current supply.

3.2. COGGING TORQUE AND BACK-EMF IN THE STUDIED MULTIPHASE PMSMs

3.2.1. Analysis of the Cogging Torque

The interaction between the permanent magnets of the rotor and the stator slots generates an undesirable torque in electrical machines named cogging torque. This torque is dependent of the relative rotor – stator position and its period per revolution is given by the number of stator slots and number of magnetic poles. The cogging torque was analyzed in the step by step in time domain (TD) with the constant speed of 1/6 [rpm], corresponding to 1 mechanical degree per second.

The cogging torque periods of each machine are: 10, 9, 6.43 and 10 degrees respectively.

In the design of the PMSMs are desired reduced peak values of the cogging torque. The results show that the 5-phase and 7-phase motors have better behavior from all studied cases. Peak values of the cogging torque of each PMSM are: 4.58 [Nm], 0.95 [Nm], 1.68 [Nm] and 4.56 [Nm], respectively. It stands out that the 5-phase PMSM presents the lowest peak value of cogging torque. Because there is no geometrical difference between the 3-phase and 9-phase motors, the cogging torque of those motors is similar.

3.2.2. Analysis of the Back-EMF

The study of the inductor magnetic field and the voltage induced by this field in the phases of the stator winding, referred to as electromotive force (EMF) or counter-electromotive force (CEMF or Back EMF), was conducted on step-by-step in time domain FE models.

The analysis of Back-EMF: (1) offers information about the amplitude order value of the applied voltage on motors; (2) is required for the safety circuits, for example, the safety circuits designed for the regenerative braking in EVs, (3) is required for the electric drive system in order to optimize their operation etc.

The studied PMS machines operate as no-load synchronous generators. The circuit models are similar to those presented in the Fig. 3.3, but only contains the coil conductor and the inductance of the frontal ends of the stator winding.

The results related the spatial structure of the primary magnetic field correspond to the last time step 0.05 [sec]. The time dependence of the back-EMF concerns a time interval of 20 [ms], between 0.03 [sec] and 0.05 [sec], with the time step of 50 [μs].

The maps of the magnetic flux density and the lines of the magnetic field of the studied PMS machines are very similar. The stator armature reaches usual level of magnetic saturation. The permanent magnets are over width and so there are small areas of the rotor's magnetic core with high magnetic saturation, at the magnet's extremes.

The amplitude of Back-EMF is directly proportional with the amplitude of magnetic flux density, thus, any spatial harmonic of the magnetic flux density influences the time variation of the voltages induced in the phases of the stator winding, along with the rotational speed of the rotor, the number of turns per phase.

Due to the same stator and rotor geometries of the 3-phase and 9-phase motors, the magnetic flux density along the middle circle of the air gap are identically. All studied PMSMs have similar content of harmonics of magnetic flux density along the middle circle of the motor air gap, however the 7-phase machine has slightly lower amplitude values.

The voltages corresponding to the fundamental time harmonic of 50 [Hz] for all four machines are: 754.45 [V]; 773.25 [V]; 762.44 [V] and 786.07 [V], respectively. The total

harmonic distortion (THD) was evaluated considering all time harmonics with the amplitude over 1 % of the amplitude of the fundamental harmonic of 50 [Hz]. The THD of Back-EMF voltage for all four machines are 30.14 %, 35.33 %, 33.11 % and 39.38 %, respectively. The 3-phase machine has the lowest THD, also the highest THD presents 9-phase machine due to a lower number of slots per pole and phase.

3.2.3. Remarks

Regarding the cogging torque, the 5-phase and 7-phase motors have lower amplitudes than the 3-phase and the 9-phase motors, however, it stands out that the 5-phase PMSM presents the lowest peak to peak values of cogging torque.

The 7-phase machine has a better content of harmonics, with slightly lower amplitudes values regarding the magnetic flux density along the middle circle of the motor's air gap.

The 3-phase machine has the lowest THD of Back-EMF voltage of 30.14 %, also the 9-phase machine has the highest THD of 39.38 %, due to a lower number of slots per pole and phase.

3.3. INITIAL PHASE OF THE STATOR CURRENTS CORRESPONDING TO THE MAXIMUM VALUE OF THE ELECTROMAGNETIC TORQUE IN PMSMs

Starting from the rated currents of the analogue's induction motors, shown in chapter 1, namely 7.923 [A], 4.682 [A], 3.254 [A] and 2.817 [A], respectively, is obtained the optimal *initial phase* φ of the current corresponding to the maximum electromagnetic torque. The rated values of the currents of PMSMs are established considering the optimal initial phase φ and the rated load torque of 50 [Nm].

In the circuits associated with the field models of PMSMs are considered the following parameters, regarding the current sources: RMS value of the stator currents *I*, the initial phase φ of the current and the frequency, *f*, of 50 [Hz]. The formulas of the electric currents in the phases of the 5-phase PMSM, for example, are:

$$\begin{aligned} i_1(t) &= \sqrt{2}\cdot I\cdot \sin(2\pi f\cdot t+\varphi)\\ i_2(t) &= \sqrt{2}\cdot I\cdot \sin(2\pi f\cdot t+2\pi/5+\varphi)\\ i_3(t) &= \sqrt{2}\cdot I\cdot \sin(2\pi f\cdot t+4\pi/5+\varphi)\\ i_4(t) &= \sqrt{2}\cdot I\cdot \sin(2\pi f\cdot t-4\pi/5+\varphi)\\ i_5(t) &= \sqrt{2}\cdot I\cdot \sin(2\pi f\cdot t-2\pi/5+\varphi) \end{aligned} \tag{3.1}$$

Introducing the initial phase as a variable parameter, we obtain the dependence between the electromagnetic torque and the phase φ, from where is obtained the optimum phase value φ_{o3} = 94 [deg] corresponding to the maximum value of the electromagnetic torque, namely 88.934 [Nm], in the case of 3-phase PMSM.

For each PMSM, the investigation into the optimal phase of the reference stator currents continued, yielding the following values: φ_{o5} = 104 [deg], φ_{o7} = 110 [deg] and φ_{o9} = 115 [deg], Table 3.1. Using those values of φ, the rms values of the current supplies for all motors were optimized in order to obtain the rated value of electromagnetic torque of 50 [Nm]. Having lower values of rated currents, the Joule losses are lower in the PMSM's stator windings compared with the analogue IMs.

The mean values of the most important space harmonic of the magnetic flux density in the air gap of all studied induction motors, about 0.73 [T] - corresponding to the rated operation, represents 64.6 % of the mean value of and of the magnetic flux density of all PMSMs, about

1.13 [T]. Also, generally, the polar step coverage factor, required in the calculation of the magnetic flux, is slightly higher in case of PMSMs than IMs. Thus, is obtained the difference between the stator currents of the two types of electric motors.

Table 3.1. Initial phase φ corresponding to the maximum of the PMSMs torque for rated speed and rated PMSMs currents that correspond to the rated torque 50 [Nm]

PMSM	3-phase	5-phase	7-phase	9-phase
I [A] (rated IM currents)	7.923	4.682	3.254	2.817
$\varphi_{optimum}$ [degree]	94	104	110	115
I [A] (rated PMSM currents)	4.60	2.763	1.991	1.479

3.4. PERFORMANCES OF RATED OPERATION OF THE MULTIPHASE PERMANENT MAGNET SYNCHRONOUS MOTORS

In this subchapter are described: the maps of the magnetic flux density and the lines of the magnetic field, the time dependence and harmonics of the electromagnetic torque, the time dependence and harmonics of the stator phase one voltage (phase-to-null) and it is evaluated the efficiency of each PMSM.

The electric circuits considered for this analysis are presented in Fig. 3.3, where each phase of the motor is represented by a coil conductor associated with the geometry, having as input parameter the electric resistance per phase and an inductor representing the inductance of the frontal ends of the stator winding. Each phase is fed by a current supply described in equation (3.1) and the values of rated currents of the PMSMs, corresponding to the rated torque of 50 [Nm], are considered those presented in Table 3.2. The magnets are taken into account for losses and are represented in the electric circuit by a parallel connection between a solid conductor and a resistor with a very high value.

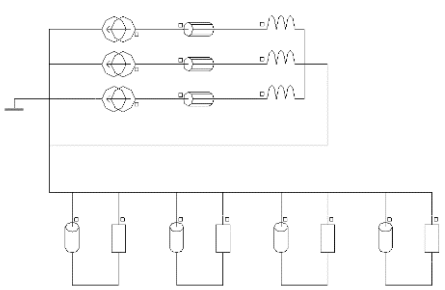

3-phase motor

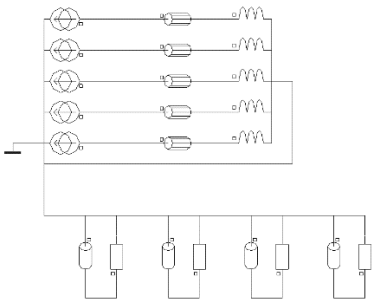

5-phase motor

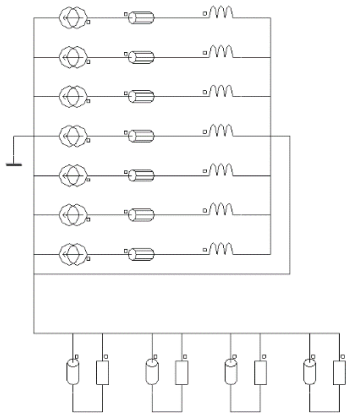

7-phase motor

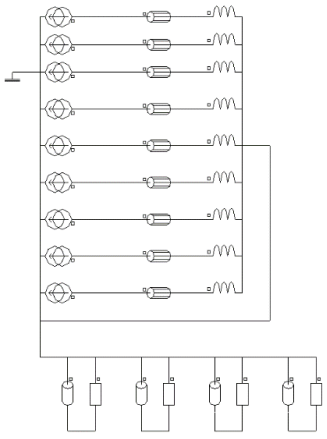

9-phase motor

Fig. 3.3. The electric circuits of the PMSMs

3.4.1. Magnetic field at rated operation and spatial harmonics of the magnetic field in the air gap

The map of the magnetic flux density and the lines of the magnetic field for the rated operation of each PMSM is shown in the extended version of the thesis.

3.4.2. Electromagnetic torque for the rated PMSMs operation

The mean values of electromagnetic torque for all PMSMs are very similar, under 1% difference, namely 49.487 [Nm], 49.451 [Nm], 49.438 [Nm] and 49.876 [Nm], respectively.

The 7-phase motor's time harmonics differs from those of the other three. The first and second harmonics of the 7-phase motor have frequencies of 1400 [Hz] and 2800 [Hz], respectively, that are significantly higher than the counterpart harmonics of the other motors. But the 7-phase motor has a lower amplitude, ~45%, for first harmonic and a lower amplitude, ~66%, for second harmonic, compared to the 9-phase motor who has the highest amplitudes of harmonics. Ripple of the electromagnetic torque for all motors are: 20.04 [Nm], 17.73 [Nm], 9.04 [Nm] and 18.23 [Nm], respectively. The 7-phase PMSM is characterized by the most reduced content of time harmonics of electromagnetic torque and the lowest level of the torque ripples.

3.4.3. Stator voltage for rated PMSMs operation

The RMS values of voltage of each PMSM are: 586.089 [V], 583.27 [V], 574.671 [V] and 619.17 [V], respectively. The amplitude of the 50 [Hz] harmonic of the stator voltage of each motor are: 821.724 [V], 816.02 [V], 802.396 [V] and 854.3 [V]. The total harmonic distortion of phase-to-null voltage are 13.41 %, 14.7 %, 16.1 % and 22.56 %, respectively. Comparing with the THD of Back-EMF, is noticeable a significant drop in THD value, about: 55.5 %; 58.4 %; 51.37 % and 42.7 %, respectively. The 3-phase PMSM presents the lowest THD of phase-to-null voltage compared to the other motors.

3.4.4. Efficiency of the PMSMs

The following formula was considered for the evaluation of the efficiency of the PMSMs:

$$Efficiency\ [\%] = \frac{Mean\ value\ \{Electromagnetic\ Torque\} \cdot Mean\ value\ \{Angular\ Speed\} - Mechanical\ losses}{Mean\ value\ \{Supply\ Active\ Power\} + Stator\ Iron\ Losses + Rotor\ Iron\ Losses} \quad (3.2)$$

The parameters from formula (3.2), where the numerator represents the mechanical power and the denominator represents the electrical power, are detailed in Table 3.2, considering the rated speed is 1500 [rpm] and the mechanical losses are imposed 5% of the first product in the equation. The magnet losses are included in supply active power.

Table 3.2. General parameters of PMSMs at rated operation

PMSM	3-phase	5-phase	7-phase	9-phase
Electromagnetic Torque [Nm]	49.487	49.451	49.438	49.876
Mechanical power [W]	7384.73	7379.36	7377.42	7442.78
Mechanical losses [W]	388.67	388.39	388.29	391.73
Supply Active Power [W]	7918.89	7907.17	7882.58	7970.14
Stator Core Losses [W]	227.14	224.23	229.02	226.721
Rotor Core Losses [W]	44.87	44.75	33.6	44.17
Electrical power [W]	8201.57	8183.86	8145.55	8251.62
Efficiency [%]	90.158	90.255	90.574	90.314

The 7-phase PMSM presents the highest evaluated efficiency, even if the highest difference between all cases is about 0.4 %. Also, the 7-phase PMSM presents slightly lower rotor core losses compared to the other cases.

3.4.5. Annotation

Total losses in the magnets for 7-phase PMSM are 0.68 W, which is very low compared to the other cases, namely 8.93 [W], 7.71 [W] and 8.9 [W], respectively. The 3- and 7-phase PMSMs are further investigated, considering an increased mesh density in the corners of the magnets for both motors for a higher precision of the results. The maps of current density in the magnet's region shows that the current density is much more concentrated in the corners in case of the 7-phase motor.

Using a sensor in the right upper corner of one magnet, was obtained the module of current density in that point for both 3-phase motor and 7-phase motor. The amplitudes of the most important harmonics are: 900 [Hz] / 844097 [A/m^2] and 1400 [Hz] / 404370 [A/m2], respectively. The mean value of current density of the 7-phase PMSM, 2.615e5 [A/m^2], represents 47.3 % from the mean value of current density value of 3-phase PMSM, 5.53e5 [A/m^2]. Also, the frequencies corresponding to the highest amplitude of the current density are proportional with the number of stator slots.

The mean value of magnetic flux density in the middle of one magnet in case of the 7-phase PMSM, 1.0365 [T], represents 98.08 % from the mean value of magnetic flux density of 3-phase PMSM, 1.0568 [T]. Also, the mean value of rotor core losses of 7-phase PMSM represents 74.9 % from the mean value of rotor core losses of 3-phase PMSM.

Considering the above statements and the influence of the magnetic flux density harmonics, which are much lower in case of 7-phase model, the total magnet's losses are admissible.

3.5. REMARKS

The finite element analyses of the multiphase permanent magnet synchronous motors with 3-phase, 5-phase, 7-phase and 9-phase of the stator winding, whose stators are identical with the stators of the analogues induction squirrel-cage motors, with the same values of the rated torque and synchronous speed, represent quantitative confirmations of the better performances of the PMSMs over the IMs.

Regarding the cogging torque, the 5-phase and 7-phase motors have better behavior than the 3-phase and the 9-phase motors, however, it stands out that the 5-phase PMSM presents the lowest peak value of cogging torque. The 7-phase machine has a better content of harmonics, with slightly lower values of the amplitudes regarding the magnetic flux density along the middle circle of the motor air gap.

The 3-phase machine has the lowest THD of Back-EMF voltage, also the 9-phase machine presents the highest THD due to a lower number of slots per pole and phase. Also, the 3-phase PMSM presents the lowest THD of phase-to-null voltage compared to the other motors.

The mean values of electromagnetic torque for all PMSMs are very similar, under 1% difference. However, the 7-phase PMSM is characterized by the most reduced content of time harmonics of electromagnetic torque and the lowest level of the torque ripples.

The 7-phase PMSM presents the highest evaluated efficiency from the four analyzed models in what concerns the number of phases on the PMSM stator winding.

Overall, the 7-phase PMSM presents the best performances from all studied cases analyzed at rated torque and speed.

CHAPTER 4. THE DESIGN OF A 5-PHASE SQUIRREL-CAGE INDUCTION MOTOR

In this chapter are presented formulas for the analytical design of a 5-phase induction motor, providing quantitative values of the motor performances and a finite element analysis for qualitative values of its performances. The objective is to design the stator core with the imposed gauge data, in order to build a physical model of a 5-phase IM.

As shown in subchapter 2.1.2, the 5-phase IM should be considered (1) steady state tolerant under up to two non-adjacent open phases fault and (2) starting tolerant with one open phase fault, shown in subchapter 2.2.2. The case of the failure of a single phase of the winding can cover most applications in which the motor can be used. Thus, an operating point is proposed for continuous operation under an open-phase fault, considering the criterion of similar value of stator Joule losses to those in healthy operation.

Within The National Institute for R&D in Electrical Engineering ICPE-CA (INCDIE ICPE – CA), the main objective of two projects were to design and manufacture a five phase motor and a dedicated drive.

Some results presented in this chapter can also be found in the author's paper [57].

4.1. ASSUMPTIONS FOR PRELIMINARY MOTOR DESIGN

The implementation team of the project established the use a commercial electric motor, from which *the stator core will be replaced with one custom made* in INCDIE ICPE – CA. Following correspondence with the manufacturer, the main overall dimensions were established on the basis of which the stator core was design.

The known data are the gauge data, without details such as the rotor slot, so were used the formulas and criteria design from [58] to design both stator and rotor core of the 5-phase IM.

4.2. THE NUMERICAL MODEL BASED ON ANALYTICAL FORMULAS OF THE 5-PHASE IM

The numerical model of the motor was realized in MATLAB, using the analytical formulas of the circuit model of IM from [58], [59] and [60]. The design of the rotor slots was unknown, thus, the rotor slot was design considering the criteria from subchapter 4.2.1. Preliminary data for the 5-phase motor are shown in Table 4.1.

Table 4.1. Preliminary data for the five-phase IM

Parameter	Value
Rated power [kW]	5.5
Line voltage supply	100 V – 50 Hz
No. of phases	5
No. of poles	4
No. of rotor slots	28
Inner diameter of the stator core[mm]	103
Outer diameter of the stator core [mm]	170.2
Length [mm]	180

4.2.1. Verification criteria

After several iterations of analytical and numerical computation, the main quotas of stator and rotor sheets was reached, they are presented in **Annex 2** and **Annex 3,** shown in the

extended version of the thesis. In its design, the criteria from [58] were taken into account, as follows:

a) the number of slots per pole and phase: $q_1 \geq 2$;

b) the value of stator teeth pitch (t_1) to be in the limits indicated in [58];

c) winding symmetry conditions;

d) the values of the magnetic flux density in different parts of the ferromagnetic circuit to be in the limits indicated in [58];

e) the values of the current density in the stator winding, in the rotor bar and in the short circuit ring of the rotor to be in the limits indicated in [58];

4.2.2. The analytical computation of the 5-phase motor for rated operation

The numerical model is based on the analytical formulas from [58] and [59]. Given the information from Table 4.1 and the geometric dimensions of the slots, the model provides data about the electric (e.g. current, power factor, resistance), electromagnetic (e.g. elmag. torque, power, iron losses) and mechanical parameters (e.g. shaft torque, power) at each value of the imposed slip.

The main dimensions of the short circuit ring are: outer diameter of 101.5 [mm], inner diameter of 62 [mm] and the height of 12 [mm]. Using the formulas from [61], the inductance of the portion of the end rings between two adjacent bars is: $L_r = 9.529e - 09\ [H]$.

For p = 2 and $q1$ = 2, the winding factor increases with the number of stator phases. The winding factor of the 5-phase IM is 0.9836. Comparing the winding factor of a 3-phase IM with a 5-phase IM, is noted an increase with roughly 3 %.

In order to manufacture a simpler and symmetrical winding, the number of turns in a slot is an integer, $n_{c1} = 14$, thereby the number of turns per phase is: $w_1 = 56$.

Using six conductors in parallel ($a_p = 6$) with the diameter of $d_{Cu} = 0.75\ [mm]$, the resistance on the stator winding phase at 115 ºC is $R1_{115°C} = 0.318\ [\Omega]$. The stator winding reactance is $X1 = 0.537\ [\Omega]$.

The magnetic flux density in the air gap was calculated using the algorithm from [59], the starting value of the tooth saturation factor $ksd = 1.4$. The algorithm stops when the error between the values of $ksd(i-1)$ and $ksd(i)$ is less than 0.1 %. The final value of the magnetic flux density in the air gap is $B_\delta = 0.6418\ [T]$, corresponding to $ksd = 1.53772$.

In order to compare the results of the numerical model based on the analytical formulas with the results of the FE model, the same value of the rotor speed was imposed, namely 1438.7 [rpm], corresponding to the slip value $s = 0.040867$. For this slip value, the rotor winding resistance relative to stator winding is $R'_2 = 0.2097\ [\Omega]$ and the rotor winding reactance relative to stator winding is $X'_2 = 0.5728\ [\Omega]$. The results are presented in Table 4.2.

4.3. THE FINITE ELEMENT COMPUTATION OF THE 5-PHASE IM

A finite element frequency domain (*FD*) analysis and a step-by-step in time domain (*TD*) analysis of the five phase squirrel-cage induction motor, previously computed with the analytical formulas, are investigated in this subchapter. The skewing effect of the rotor was not considered.

The full geometry and the mesh distribution of the 2D FE model, in which there are considered $140 \cdot 10^3$ of elements (with the remark that there are used second order elements), are presented in Figs. 4.1 – 4.2.

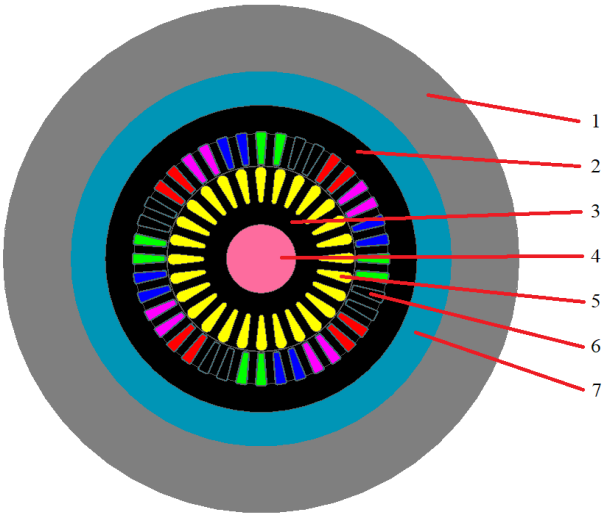

Fig. 4.1. Full geometry of the 2D FE model
(1 – infinite box; 2 – stator sheet; 3 – rotor sheet; 4 – shaft; 5 – rotor slot; 6 – stator slot; 7 – non-conductive region) [57]

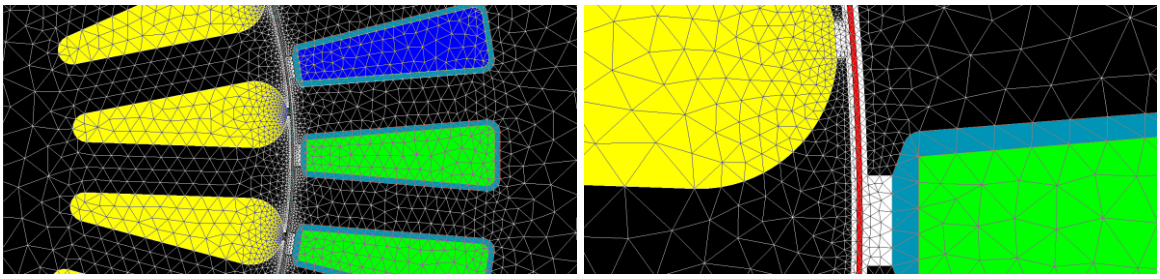

Fig. 4.2. Mesh distribution of the model [57]

The electric circuit associated to the field model of IM is shown in Figure 4.3. In the formulas (4.1) are described the electric voltages, where U_{ph} represents the RMS value of the stator voltage per phase and f represents the frequency which is considered constant in this study with the value of 50 [Hz]:

$$\begin{aligned} u_1(t) &= \sqrt{2} \cdot U_{ph} \cdot \sin(2\pi f \cdot t) \\ u_2(t) &= \sqrt{2} \cdot U_{ph} \cdot \sin(2\pi f \cdot t - 2\pi/5) \\ u_3(t) &= \sqrt{2} \cdot U_{ph} \cdot \sin(2\pi f \cdot t - 4\pi/5) \\ u_4(t) &= \sqrt{2} \cdot U_{ph} \cdot \sin(2\pi f \cdot t - 6\pi/5) \\ u_5(t) &= \sqrt{2} \cdot U_{ph} \cdot \sin(2\pi f \cdot t - 8\pi/5) \end{aligned} \tag{4.1}$$

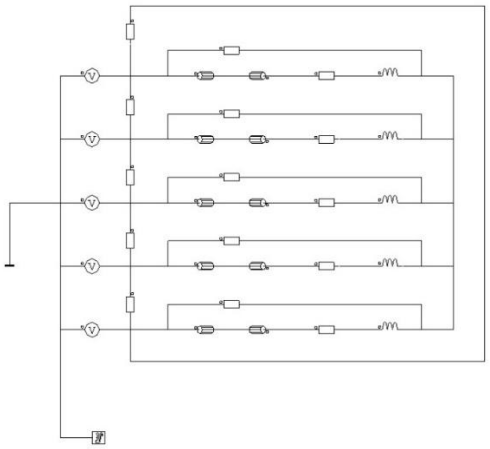

Fig. 4.3. Electric circuit of the five-phase motor

4.3.1. Healthy operation of the computed 5-phase IM

The rotor motion in relation to the stator is not taken into account in the *magneto-harmonic model in frequency domain* (*FD Model*) of the induction machine, also the slip value is imposed for this type of application [62]. Using a parameterized magneto-harmonic model with different rotor-stator relative positions, the position at which the instantaneous value of the electromagnetic torque is equal to its average value can be determined.

For the slip value of 0.04, the angular step value is 0.25 degrees over a single period. The electromagnetic torque is closer to its average value at the resulting angle of 4.5 degrees. This angular position value is therefore utilized in the subsequent frequency domain studies.

The magnetic field harmonics due to rotor-stator relative positions, also due to the slotting of stator and rotor are analyzed in the *TD* model. The relationship between the speed of the rotor and the electromagnetic torque, Fig. 4.4, was evaluated considering the following:

- the model has imposed speed in order to evaluate the electromagnetic torque at each step;
- a step of 25 [rpm] is used for the speed range 1500 ÷ 1000 [rpm] and a step of 50 [rpm] is used for 1000 ÷ 0 [rpm];
- each imposed-speed application is evaluated for 0.4 [s], for a faster transition to steady state, the first half of the period is using a step of 1.5 [ms] and the other half is using a step of 1 [ms];
- for each application, the electromagnetic torque is evaluated over two periods corresponding to the rated frequency, namely 0.04 [s].

For the speed range 1450 ÷1275 [rpm] it is attained a difference less or equal than 3.5 %. For the speed value of 1400 [rpm] it is obtained a difference of 0.71 % and for 1375 [rpm] it is obtained a minimum difference of -0.56 %.

The following formulas [63] were used to calculate the output power of the IM:

$$P_{J1} = 5 \cdot R_1 \cdot {I_1}^2 \tag{4.2}$$

$$P_{J2} = s \cdot \left(P_1 - P_{J1} - P_m\right) \tag{4.3}$$

$$P_2 = P_1 - P_{J1} - P_{J2} - P_m - P_{mech} \tag{4.4}$$

$$T_{shaft} = \frac{60 \cdot P_2}{2 \cdot \pi \cdot n} \tag{4.5}$$

where, P_{J1} – stator Joule losses, P_{J2} – rotor Joule losses, R_1 – mean value of phases resistances, I_1 – mean value of stator currents, P_1 – mean value of the active power from power sources, P_2 – the output power of IM, P_m – iron losses and T_{shaft} – shaft torque. It was considered the mechanical losses, $P_{mech} = 0.05 \cdot P_2$.

The variation of the output power with respect with the rotor speed, for both types of models, are presented in Figs. 4.5.

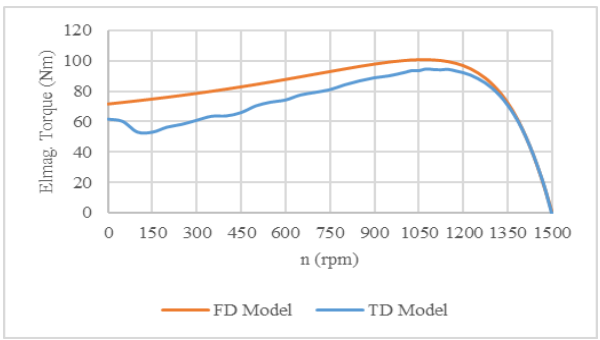

Fig. 4.4. The electromagnetic torque dependence with the rotor's speed [57]

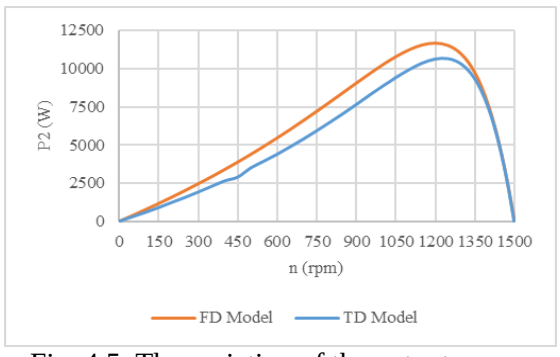

Fig. 4.5. The variation of the output power with the rotor speed [57]

An additional imposed-speed application with a speed value of 1438.7 [rpm] was evaluated for a closer look at the rated operation of the IM. A 50 [μs] time step was used for this application. The time dependence of the electromagnetic torque and of the stator currents are depicted in Figs. 4.6 and 4.7, respectively.

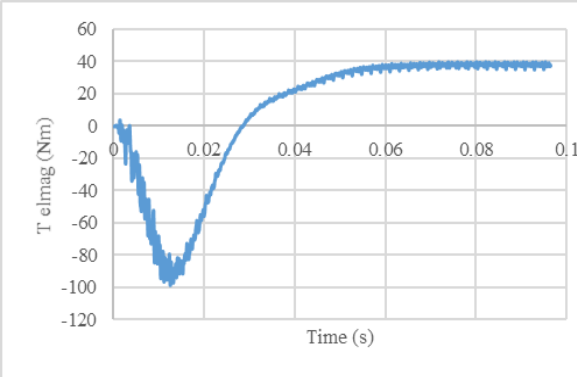

Fig. 4.6. The electromagnetic torque's time dependence [57]

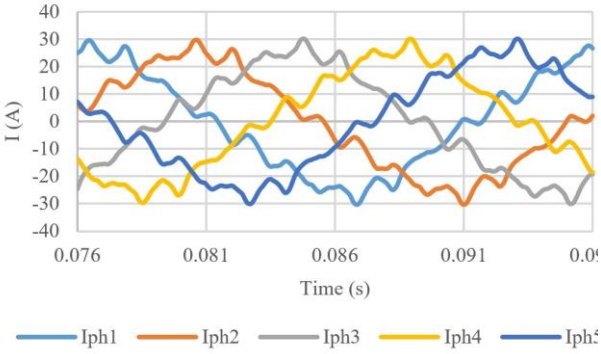

Fig. 4.7. The stator currents' time dependence [57]

The electromagnetic torque has a mean value of 38.1 [Nm] and a torque ripple of 4.97 [Nm] (13.05 %). The most significant harmonics of the electromagnetic torque are: 1450 [Hz] / 1.062 [Nm], 950 [Hz] / 0.54 [Nm], 1000 [Hz] / 0.336 [Nm] and 90 [Hz] / 0.134 [Nm].

The stator currents have the mean RMS value of 17.062 [A]. The THD of currents is slightly high because the rotor's skewing effect was not taken into account, namely 14.02 %. The most significant harmonics of the stator currents that are: 150 [Hz] / 2.05 [A], 600 [Hz] / 1.751 [A], 650 [Hz] / 1.367 [A] and 800 [Hz] / 0.89 [A].

The rated operation parameters of the studied IM are presented in Table 4.2. The reference model in the calculation of the difference in results is represented by the *TD* model.

Table 4.2. The rated operation parameters of the 5-phase IM

Model	n	T_{elmag}	I_1	P_1	P_{J1}
	[rpm]	[Nm]	[A]	[W]	[W]
(1) FD	1438.7	36.731	17.151	6388.244	467.464
(2) TD	1438.7	38.1	17.062	6626.632	462.652
(3) Analytical	1438.7	38.215	18.587	6795.455	549.036
Diff. [%] (2-1)	0	3.593	-0.522	3.597	-1.04
Diff. [%] (2-3)	0	-0.302	-8.938	-2.548	-18.671
Model	P_{J2}	P_{mech}	P_2	T_{shaft}	Efficiency (η)
	[W]	[W]	[W]	[Nm]	[%]
(1) FD	220.28	266.239	5324.786	35.343	83.353
(2) TD	219.28	276.315	5526.298	36.681	83.395
(3) Analytical	291.925	267.426	5190.996	34.455	82.804
Diff. [%] (2-1)	-0.456	3.647	3.646	3.648	0.05
Diff. [%] (2-3)	-33.129	3.217	6.067	6.069	0.709

For this value of imposed speed, the differences between the *FD* and *TD* models are relatively small, ~ 3.6 %, given that the *FD* model only considers the fundamental frequency. Although, the analytical model has the fastest computational time, the differences between this model and the *TD* model are relatively large. This model cannot predict the stator phase current and the Joule losses in the rotor. Further investigations will be carried out on the parameters that predicts the phase current and Joule losses in the rotor cage.

4.3.2. One open-phase fault operation of the computed 5-phase IM

There are critical systems that require the motors to run continuously, like the cooling fluid recirculation pump of a system or in some glass factories, where the production's performances can slow down without being easily interrupted.

Regarding the failure of the electric supply, open phase fault, a multiphase induction motor has the ability to operate under this faulty conditions. A five phase induction motor can operate under one open-phase fault during operation and start-up, as shown in [54] and [64].

For the electromagnetic torque dependence with the rotor speed of the IM under one open-phase fault operation, Fig. 4.8, the *FD* models were used.

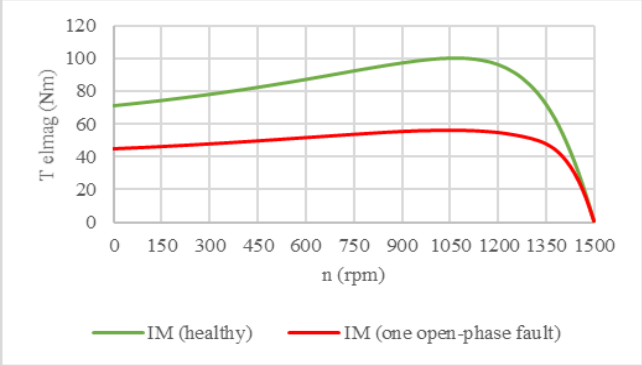

Fig. 4.8. The electromagnetic torque dependence with the rotor's speed for healthy operation and one open-phase fault operation [57]

A significant decrease in electromagnetic torque is noted, the four out of five powered phases of the IM provide up to 56.2 % of healthy operation near the maximum point and up to 63.2 % of starting torque.

An operation point is proposed for continuous operation under one open-phase fault considering the value of stator Joule losses comparative with its value corresponding to the rated operation of the healthy IM. A quasi-uniform temperature distribution is provided by the iron core, this being an integrative medium. In this manner, it tends to keep a comparative temperature in various parts of the motor, compared to the healthy one and it can maintain the insulation health until maintenance.

An additional imposed-speed application with a speed value of 1445.5 [rpm] was evaluated for a closer look at the continuous operation under one open-phase fault of the IM. A 50 [μs] time step was used for this application. The time dependence of the electromagnetic torque and of the stator currents are depicted in Figs. 4.9 and 4.10, respectively.

The electromagnetic torque has a mean value of 31.39 [Nm] and a torque ripple of 26.1 [Nm] (83.27 %). The four harmonics of the electromagnetic torque that are most significant are: 100 [Hz] / 10.04 [Nm], 575 [Hz] / 2.38 [Nm], 775 [Hz] / 1.32 [Nm], and 875 [Hz] / 1.03 [Nm]. The stator currents have the RMS value of 22.682 [A], 15.752 [A], 17.176 [A] and 22.02 [A], respectively. Also, the THD values are 9.03 %, 14.386 %, 16.76 % and 12.28 %.

The two studied cases, healthy operation and continuous operation under one open phase fault, time domain applications, are compared in Table 4.3. For maintaining the same value of the stator Joule losses, it is noted an increase of the mean value of the stator currents by ~ 10%, of the Joule losses in the rotor bars and a decrease of the output power by ~ 21 %.

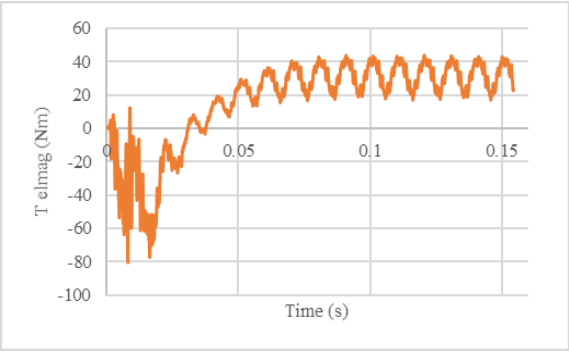

Fig. 4.9. The electromagnetic torque's time dependence for one open fault operation [57]

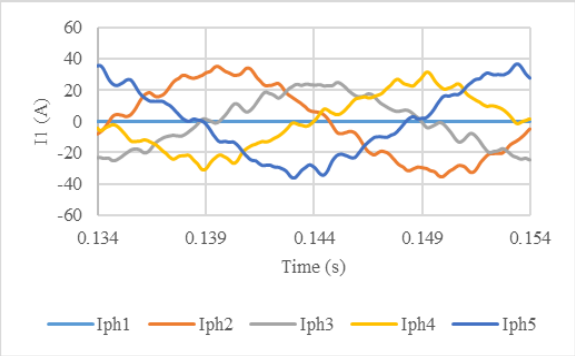

Fig. 4.10. The stator currents' time dependence for one open fault operation [57]

Table 4.3. The healthy operation parameters and continuous operation under one open-phase fault parameters of the IM

Case	n	T_{elmag}	I_1	P_1	P_{J1}
	rpm	Nm	A	W	W
Healthy	1438.7	38.1	17.062	6626.632	462.652
One open phase fault	1445.5	31.391	19.07	5639.077	462.343
Diff. [%]	0.47	-21.372	10.53	-17.513	-0.067
Case	P_{J2}	P_{mech}	P_2	T_{shaft}	Efficiency (η)
	W	W	W	Nm	%
Healthy	219.28	276.315	5526.298	36.681	83.395
One open phase fault	245.32	228.412	4568.248	30.179	81.011
Diff. [%]	10.613	-20.972	-20.972	-21.545	-2.943

4.4. REMARKS

For the imposed value of the rotor speed, the differences between the *FD* and *TD* models of the healthy 5-phase IM are relatively small, ~ 3.6 %, given that the *FD* model only considers the fundamental frequency. Although, the analytical model has the fastest computational time, the differences between this model and the *TD* model are relatively large. This model cannot predict the stator phase current and the Joule losses in the rotor. Further investigations will be carried out on the parameters that predicts the phase current and Joule losses in the rotor cage.

Considering the similar value of stator Joule losses between healthy operation and one open-fault operation of the 5-phase IM, it is observed a drop in output power of ~ 21 %, additionally, a rise in rotor bar Joule losses and stator currents by roughly 10 % and a drop in efficiency of ~ 3 %. A similar study can be conducted by substituting the voltage sources with current sources and restricting phase current to the rated value, thus maintaining the same current density per phase.

The torque ripple has increased by 5.25 times for the IM's operating under one phase fault and the 100 [Hz] harmonic's amplitude has significantly increased. The amplitude of the 100 [Hz] represents roughly ~ 30 % of the mean value of the electromagnetic torque, similarly to the one open-phase fault operation of the 5-phase IM presented in the subchapters 2.1.2.2. and 2.2.2.

CHAPTER 5. THE MANUFACTURING AND TESTS OF A PHYSICAL 5-PHASE SQUIRREL-CAGE INDUCTION MOTOR

In this chapter are presented the manufacturing process the stator laminated stack, the winding process of the stator, the test bench and the results measured on the physical 5-phase squirrel-cage induction motor.

5.1. MANUFACTURING THE STATOR LAMINATED STACK

The stator sheets were made on the basis of the drawing in **Annex 2**, presented in the extended version of the thesis. Those were placed on a packing mandrel and consolidated.

5.1.1. Manufacturing the stator sheets

The stainless-steel sheets cutting was performed in nitrogen gas for minimal local deformation of the material. The catchment to the support table of the material was made in six points, in order to reduce material vibration. In Figure 5.1 are shown the stator sheets made.

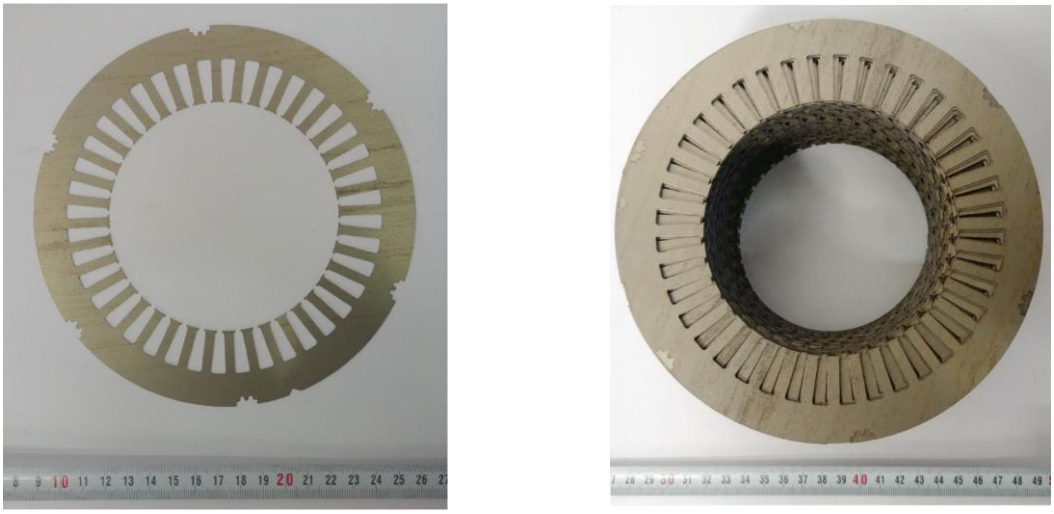

Fig. 5.1. Stator sheets manufactured

5.1.2. Packing the stator sheets on the mandrel

The sketch of the packing mandrel is shown in Fig. 5.2.

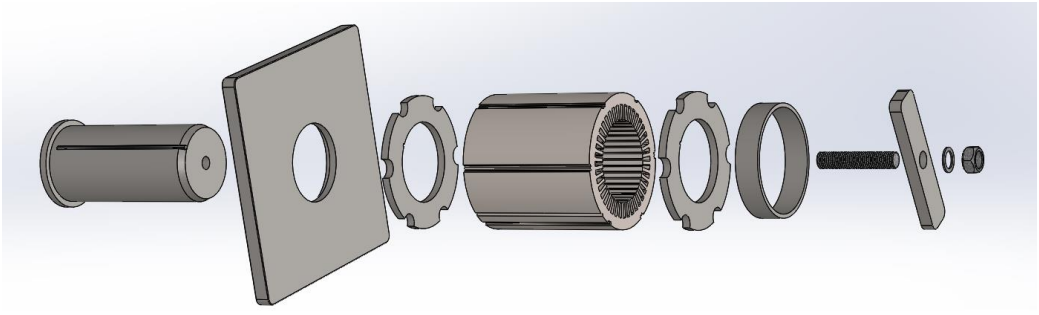

Fig. 5.2. The sketch of the packing mandrel

5.1.3. Mechanical consolidation of the stator laminated stack

As can be seen in Figure 5.3, there is a significant variation in the outer diameter of the sheets, due to the vibration of the sheet in the cutting process which led to deviations in dimensions. Thus, it is necessary to rectify it so that it is inserted into the housing of a commercial motor. Such grinding will be done on the lathe, so the package must be rigid enough

so that it does not fall apart. The stiffening solution chosen is welding, representing a compromise between good stiffening and additional iron losses.

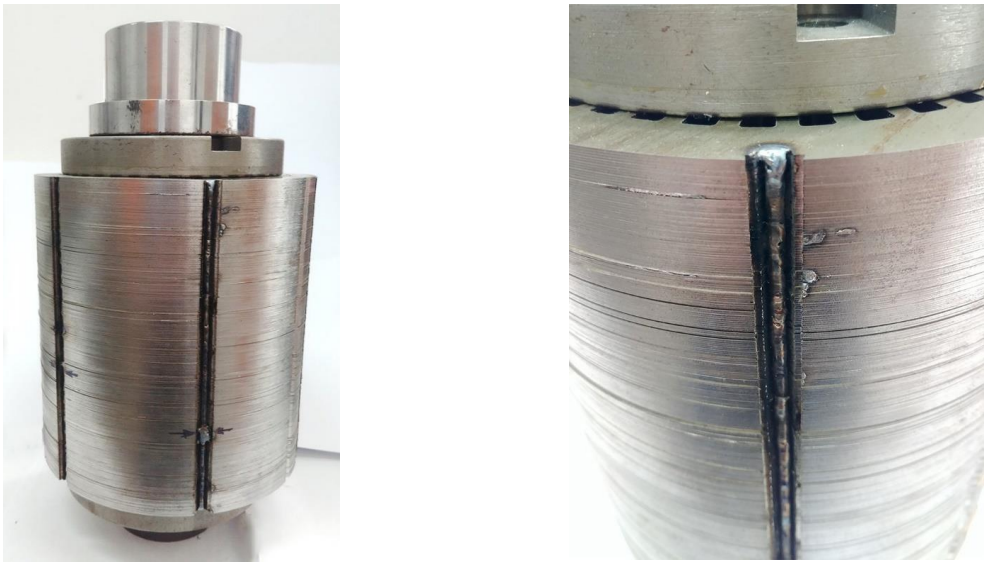

Fig. 5.3. Stator laminated stack

5.2. WINDING THE STATOR CORE AND THE ASSEMBLY OF THE MOTOR

The exterior of the stator laminated stack was rectified by S.C. ELECTROPRECIZIA S.A. and it was put in the motor housing. The design of the rotor slots is unknown. Assuming that the rotor slot area is lower than the case presented in chapter four, the number of turns per phase has been reduced from 56 to 44. The stator winding scheme used for the physical model in presented in **Annex 4**, shown in the extended version of the thesis. The winding process of the stator core started by inserting the slot insulation. In Fig. 5.4 is shown the half-way process of the stator winding.

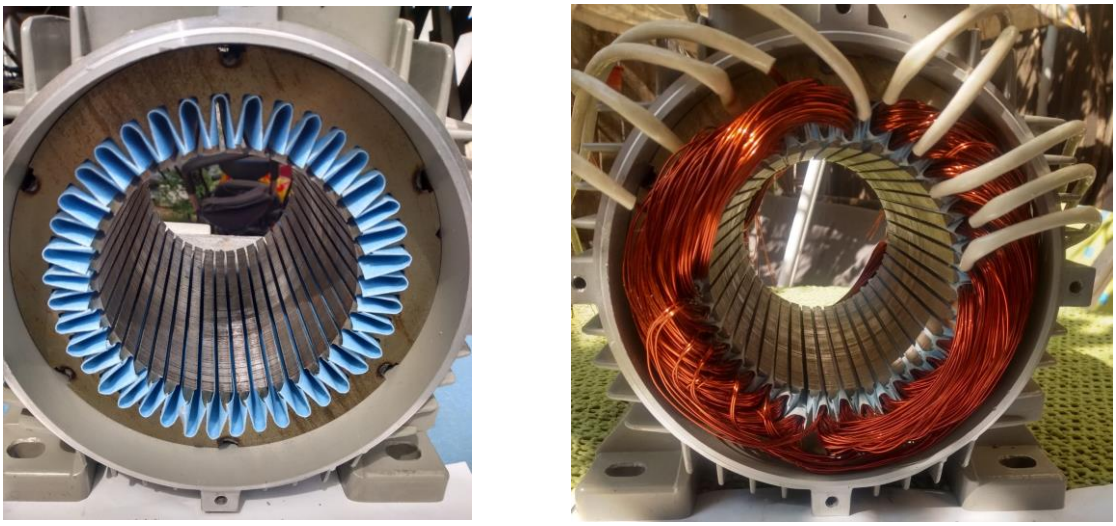

Fig. 5.4. The half-way process of the stator winding

The stator winding of the physical model is presented in Fig. 5.5. Due to some technical difficulties, an extra layer of protection was added for the front ends of the winding, being a prototype model, the motor will be disassembled several times. The fully assembled five phase physical model is presented in Fig. 5.6.

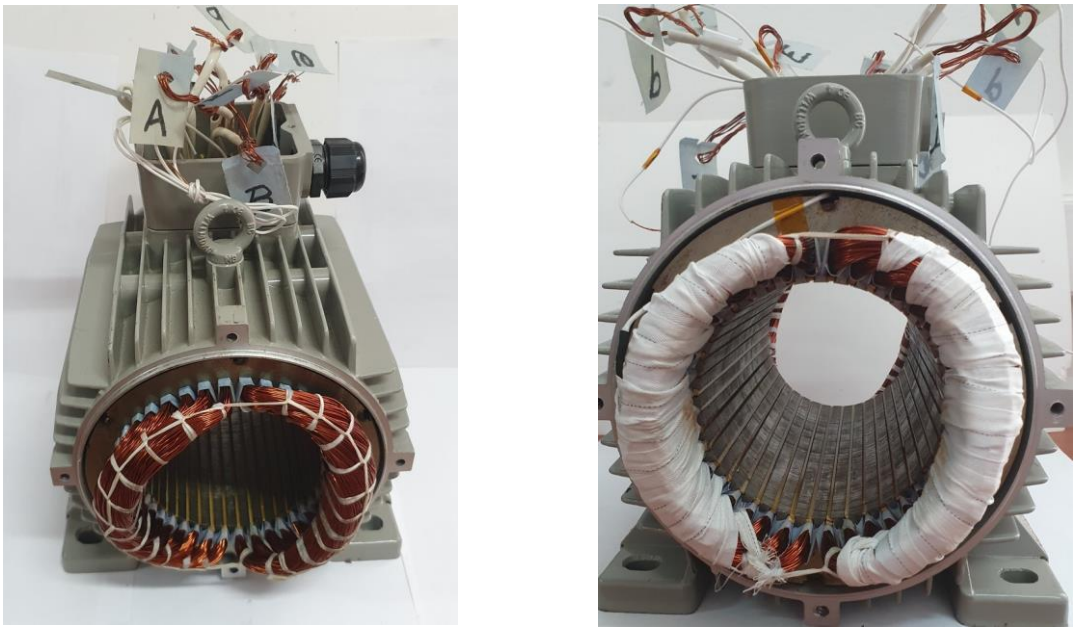

Fig. 5.5. The stator winding of the physical model

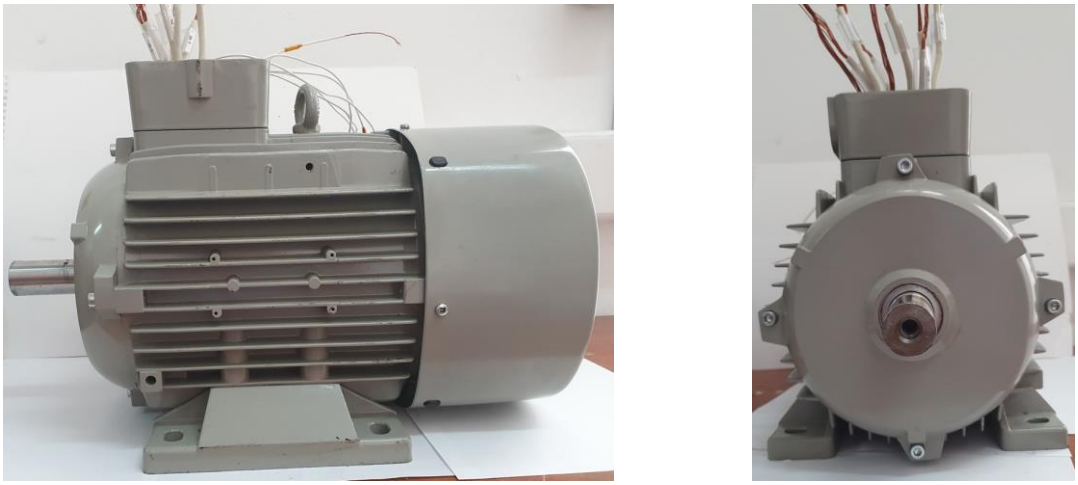

Fig. 5.6. Fully assembled five phase physical model

5.3. EXPERIMENTAL TESTS AND RESULTS

5.3.1. Checking the insulation between the housing and the phase

After the physical model was fully assembled, the checking the insulation between the housing and each phase was performed at different values of voltage, namely 50 [Vcc] / 55 [MΩ], 100 [Vcc] / 110 [MΩ], 500 [Vcc] / 500 [MΩ]. The tests were performed using the apparatus: Sefram 9091 Insulation Multimeter.

5.3.2. Phase resistance measurement

The phase resistance was measured at the room temperature of ≈ 26ºC and with a value of the current of 1 [A]. The mean value of phase resistance is 0.141366 [Ω]. The resistance of each phase don't exceed 1 % (0.866 %) difference compared with the mean value. The tests were performed using the apparatus: Extech Industries UM200.

5.3.3. The bench test

For testing the physical model of induction motor, a direct current motor of 7 [kW] was borrowed from the National University of Science and Technology POLITEHNICA Bucharest. This was used as a generator, feeding the excitation winding and providing mechanical power.

In Figure 5.7 is presented the diagram of the bench test and in Fig. 5.8 is shown the physical bench test. The alternating current from a three phase power supply passes through a three phase auto transformer, it is rectified and filtered before reaching the custom made 5-phase inverter which feeds the physical model of the 5-phase IM.

The alternating current from a one-phase power supply passes through an auto transformer, it is rectified and it is feeding the excitation of the DC generator. Together with the output power of the 5-phase IM, the output power of the DC generator passes through a load resistance.

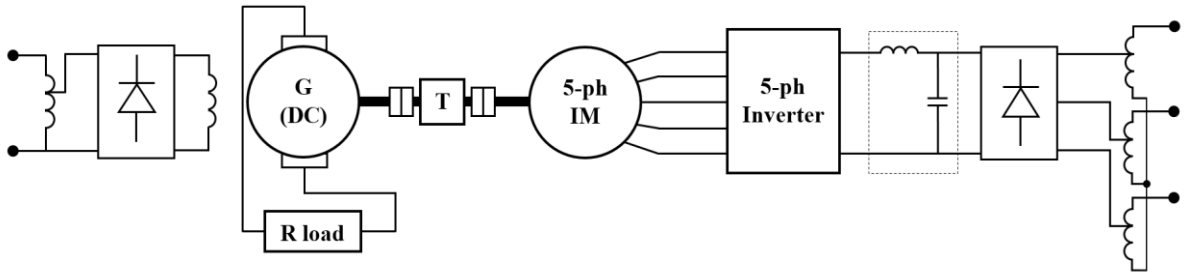

Fig. 5.7. The diagram of the bench test

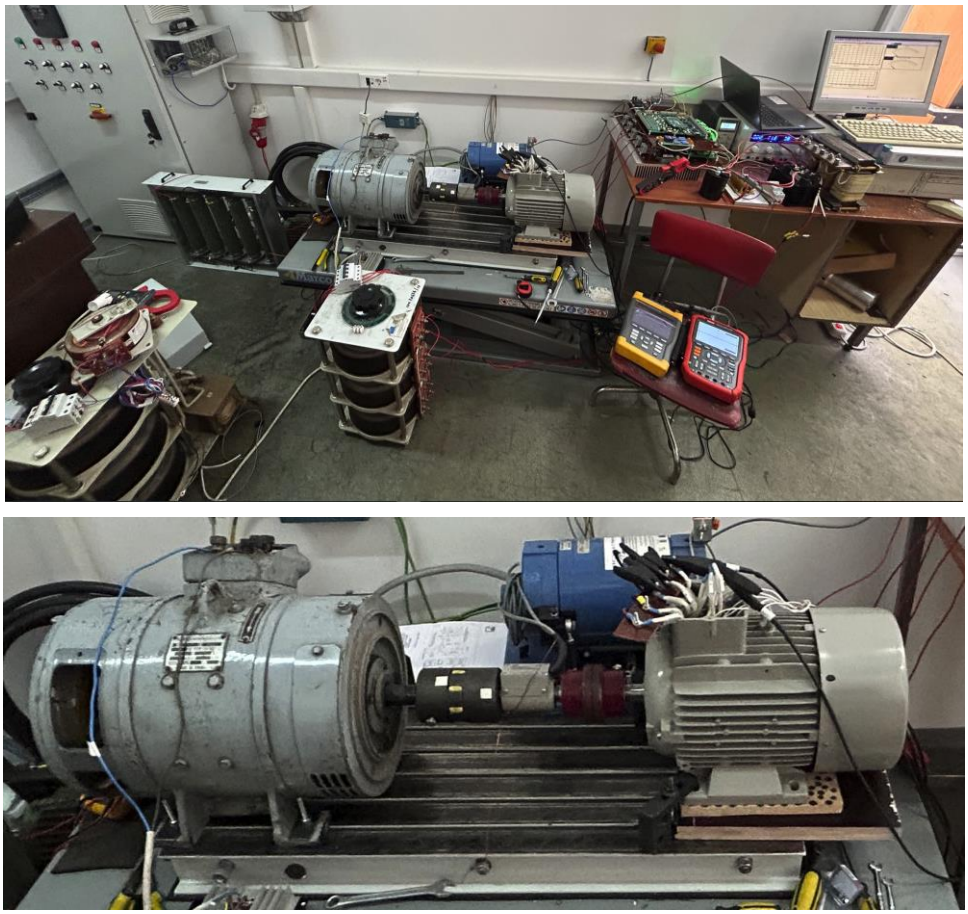

Fig. 5.8. The bench test

The name of the measuring apparatus used are shown in the extended version of the thesis.

5.3.4. Healthy operation of the physical model of 5-phase IM

The parameters measured on the physical model of the inverter and on the 5-phase IM, the full chain of results are founded in the **Annex 5**, presented in the extended version of the thesis. The efficiency of the 5-phase system (inverter and IM) was calculated dividing the output mechanical power of the IM by the input electrical power of the inverter.

With the available equipment at this moment, it was not possible to correctly measure the value of power factor, due to PWM voltage.

In Fig. 5.9 – 5.12 are shown the correspondence between speed shaft torque, mechanical power, phase current and efficiency of the system.

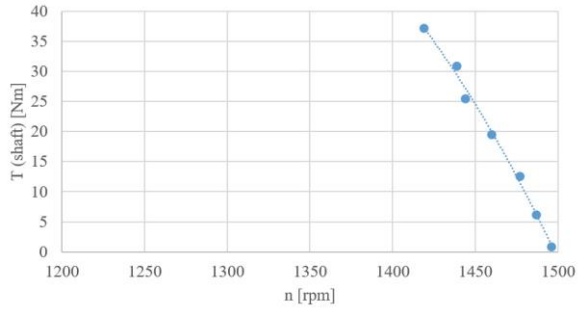

Fig. 5.9. The dependence of the torque with the speed

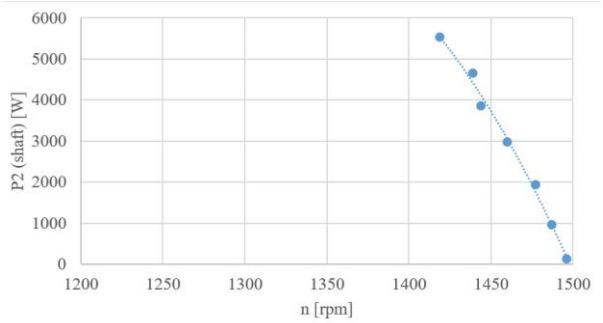

Fig. 5.10. The dependence of the output power with the speed

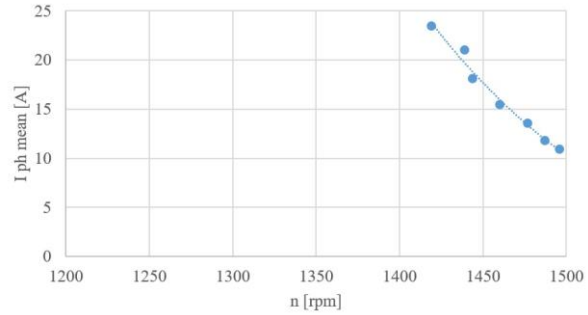

Fig. 5.11. The dependence of the phase current with the speed

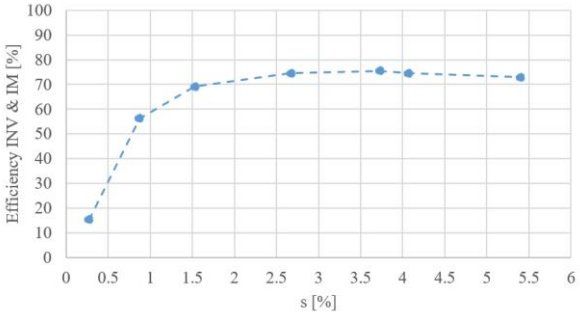

Fig. 5.12. The dependence of the system's efficiency with the slip

The waveforms of the phase A current's are shown in Fig. 5.13, corresponding to the no load operation, with the shaft of the DC generator coupled and no excitation. Also, at load operation of 5.5 [kW], the waveform is shown in Fig. 5.15.

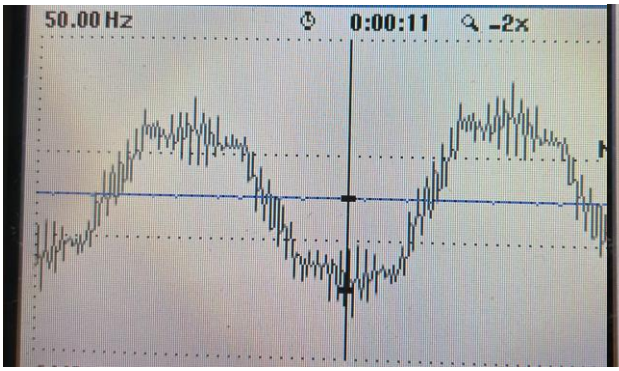

Fig. 5.13. The waveform of the phase A current's at no load operation

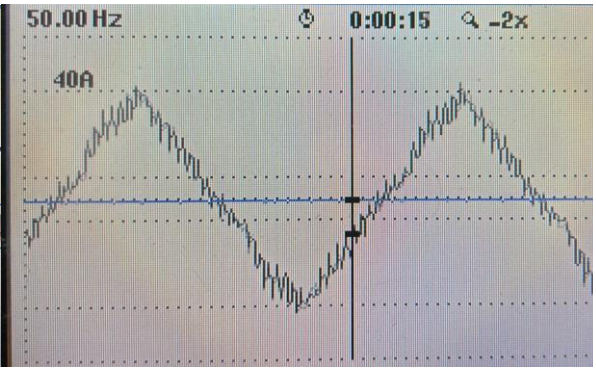

Fig. 5.15. The waveform of the phase A current's at load operation

The waveforms of the stator currents of the physical model will be improved firstly by implementing an improved drive command.

5.3.5. One open-phase fault operation of the physical model of 5-phase IM

In chapter four (subchapter 4.3.2), an operation point is proposed for continuous operation under one open-phase fault considering the value of stator Joule losses comparative with its value corresponding to the rated operation of the IM. In Table 4.3 is shown that a drop in power of ~ 21 %, this criterion is met.

For this test, the **phase E** was disconnected. The excitation winding of the DC generator was not powered for the no load operation measurement. For the load operation measurement, the excitation winding voltage of the DC generator was gradually increased until the shaft torque reached ~ 80 % of the healthy rated operation.

In Table 5.5 are presented the parameters measured on the physical model of the inverter and on the IM with four out of five phases fed, those results can be founded in the **Annex 5**.

Table 5.5.a. The measured parameters on one open-phase fault operation of the physical model of 5-phase IM

Nr. crt.	U [Vcc]	I [A]	P (INV) [W]	I ph 1 [A]	I ph 2 [A]	I ph 3 [A]	I ph 4 [A]	I ph 5 [A]	I ph med [A]
1	204.2	7.17	1464.11	17.2	14.2	12.5	16.4	-	15.08
2	204	28.2	5752.8	28.5	22.6	18.5	28.8	-	24.6

Table 5.5.b. The measured parameters on one open-phase fault operation of the physical model of 5-phase IM

Nr. crt.	n [rpm]	s [%]	T shaft [Nm]	P2 (shaft) [W]	Efficiency INV & IM [%]
1	1496	0.27	0.82	128.46	8.77
2	1439	4.07	29.5	4445.41	77.27

5.3.6. Remarks

The open-phase fault operation process differs slightly from that presented in subchapter 2.1.2.2, where the 5-phase IM operates at rated torque and after the steady state is reached, one phase is interrupted. However, the functionality under one open-phase fault operation of the physical model of five phase IM is validated in this subchapter.

The waveforms of the stator currents of the physical model will be improved firstly by implementing an improved drive command.

5.4. THE DIRECTION OF ROTATION FOR A 5-PHASE MOTOR

An electric motor has an advantage of reversing the direction of rotation, for example, a three phase motor will change the direction of rotation by switching any two feeding phases of the motor. The change the direction of rotation of a five phase motor is not mentioned in the literature, in the view of the author's search. Because the DC Generator used for testing the IM is unidirectional, the change of the direction of rotation of the 5-phase IM was necessary for the test bench. In the extended version of the thesis, the process by which the direction of rotation of the 5-phase machine can be changed is presented.

5.5. REMARKS

The physical model of the 5-phase IM represents a proof of concept and the experimental results are a quantitative validation of its functionality. By improving the 5-phase IM and drive, also the different elements in the test bench (like filter parameters), will be obtain a qualitative validation of the five phase system.

The open-phase fault operation process differs slightly from that presented in subchapter 2.1.2.2, where the 5-phase IM operates at rated torque and after the steady state is reached, one phase is interrupted. However, the functionality under one open-phase fault operation of the physical model of 5-phase IM is validated in this chapter.

The waveforms of the stator currents of the physical model will be improved firstly by implementing an improved drive command.

With the available equipment at this moment, it was not possible to calculate the value of power factor.

Regarding the changing the direction of rotation, different cases have been testing on the physical model of the 5-phase IM. It was noted that for the five phase system are necessary two swipes of two phases. Examples of phases swipes: (A – C) and (D – E); (A – E) and (D – B) etc.

CONCLUSIONS

The comparison of the steady-state parameters for the rated operation point of the studied four cases of the induction motors, shows that the 7-phase presents the better overall performances. It follows the 5-phase case regarding the electric efficiency, the content of harmonics of the normal component of the magnetic flux density along a middle air gap circle and the relative starting torque.

Two types of the faults tolerance of multiphase induction motors were studied - the steady state tolerance, associated with the steady state motor's operation at rated torque and the starting tolerance associated with the motor starting at rated torque. The motors are considered to be tolerant if the values of operation parameters at the end of the transients are close to those in healthy operation.

The three-phase induction motor should be considered not steady state tolerant regarding the failure of one phase due to the increase of the torque and currents harmonics and the important torque ripples. This motor is also not starting tolerant for the one phase failure even in the case of star connection of the three phases, null accessible and four conductors electric supply.

The five-phase induction motor is steady state tolerant regarding the failures of one phase and of two non-adjacent phases, even if the torque ripples increases. This motor is starting tolerant only in the case of one phase failure.

The seven-phase induction motor is steady state tolerant to the failures of one phase, two phases, three phases and even four non-adjacent phases. In all faulty cases, the torque ripples increases. This seven-phase motor starting tolerant in cases of the failure of one phase and of two specific phases, such as Phase-1, -3; Phase-2, -4; Phase-3, -5 etc.

The nine-phase induction motor is steady state tolerant regarding the failures of one phase, two phases, three phases and four non-adjacent phases. This motor is starting tolerant in case of the failure of one phase and even of the failures of two phases.

It is observed a diminishing of the electromagnetic torque ripple with the increase of number of stator phases.

The finite element analyses of the multiphase permanent magnet synchronous motors with 3-phase, 5-phase, 7-phase and 9-phase of the stator winding, whose stators are identical with the stators of the analogues induction squirrel-cage motors, with the same values of the rated torque and synchronous speed, represent quantitative confirmations of the better performances of such type of electrical motors over the induction motors.

Regarding the cogging torque, the 5-phase and 7-phase motors have better behavior than the 3-phase and the 9-phase motors, however, it stands out that the 5-phase PMSM presents the lowest peak value of the cogging torque. The 7-phase machine has the lowest amplitudes of harmonics regarding the magnetic flux density along the middle circle of the motor air gap.

The 3-phase machine has the lowest content of harmonics of Back-EMF voltage. The 3-phase PMSM presents the lowest THD of the phase-to-null voltage compared to the other motors. The 9-phase machine presents the highest THD of Back-EMF voltage due to a lower number of slots per pole and phase, q = 1.

The mean values of electromagnetic torque for all PMSMs are very close, under 1% difference. However, the 7-phase PMSM is characterized by the most reduced content of time harmonics of electromagnetic torque and the lowest level of the torque ripples, followed by the 5-phase PMSM. The 7-phase PMSM presents the highest efficiency from the four analyzed cases.

The 5-phase motor was designed and a comparison was performed of the results of the induction motor computation based on the analytical formulas and of the finite element analysis, in the frequency domain and in time domain. The comparison between the *FD* and the *TD* models shows a maximum difference of 3.65 % regarding the electromagnetic torque and the active power absorbed, which is acceptable considering that the *FD* model doesn’t evaluates the harmonics of different parameters. Also, the analytical formulas present an increase of 8.9 % in the case of stator currents, resulting also in a difference in the stator losses.

There are critical systems that require the motors to run continuously, like the cooling fluid recirculation pump of a system or in some glass factories, where the production's performances can slow down without being easily interrupted. Regarding the electric supply failure, open phase fault, a multiphase induction motor has the ability to operate under this faulty condition.

An operation point was proposed and analyzed for continuous operation under one open-phase fault considering the value of stator Joule losses is comparative with its value corresponding to the rated operation of the IM. For this operation point the output power dropped by ~ 21 % of the 5-phase IM, additionally, the rotor bar Joule losses and stator currents have increased by roughly 10%. The torque ripple has increased by 5.25 times and the 100 [Hz] harmonic's amplitude has significantly increased. A similar study can be conducted by substituting the voltage sources with current sources and restricting phase current to the rated value, thus maintaining the same current density per phase.

The description of the manufacturing of a physical model of a 5-phase squirrel-cage induction motor and of the test bench of this model are elaborated in the fifth chapter. The physical model of the 5-phase IM represents a proof of concept and the experimental results are a quantitative validation of its functionality. By improving the 5-phase IM and the drive,

also the different elements in the test bench, will be obtain a qualitative validation of the five phase system.

Unlike the finite element analysis under open-phase fault operation, that was performed at rated torque for both steady state and starting tolerance, the open-phase fault operation of the physical model of 5-phase IM was performed by gradual increase in the generator load. However, its functionality is validated.

Changing the direction of rotation, for a three phase motor, is achievable by switching any two feeding phases of the motor. For the five phase motor are necessary two swipes of two phases. Different cases have been testing on the physical model of 5-phase IM. Examples of phase swipes: (A – C) and (D – E); (A – E) and (D – B) etc.

THESIS CONTRIBUTIONS IN THE INVESTIGATION OF MULTI-PHASE ELECTRICAL MACHINES

This thesis presents a bibliographic study on multiphase machines, which highlights their advantages over three-phase machines. It completes and quantifies the fault tolerant argument, for both at start-up and when the fault occurs during operation, described in the bibliographic study. Also, it quantifies and shows a diminishing of the electromagnetic torque ripple with the increase of number of stator phases.

The implementation of the numerical finite element models, for the analysis in frequency domain and time domain, led to a comparison between 3-, 5-, 7- and 9-phase machines of both induction motors and permanent magnet synchronous motors. The stator winding schemes for the 3-, 5-, 7- and 9-phase machines (Annex 1) were designed and used in the finite element analyses.

The finite element models presented in the fourth chapter have three layers of air-gap, resulting in an increased number of nodes in the mesh distribution of the model and an increase in the quality of the results.

The design of the five phase induction motor was achieved by the implementation of the numerical model based on analytical formulas and of the numerical finite element models.

The main quotas of stator and rotor sheets (Annex 2 and 3) has been iteratively design so that the magnetic flux density in different parts of the machine comply with the recommendations from [58]. The drawing in the Annex 2 was used for manufacturing the stator laminated stack included in the physical model. The magnetic core was inserted into the casing, the stator winding was executed and led to the realization of the physical model a 5-phase IM.

The physical model of the 5-phase IM was tested with the help of a custom made 5-phase inverter.

The functionality of the 5-phase IM in the proposed continuous operation point under one open-phase fault, where the value of stator Joule losses is comparative with its value corresponding to the rated operation of the IM, was validated through experimental tests of the physical model of 5-phase IM.

Changing the direction of rotation, for a three phase motor, is achievable by switching any two feeding phases of the motor. In the case of the five phase motor are necessary two swipes of two phases.

From the studies presented in this thesis resulted four papers published in conference volumes and in ISI-listed journals, indexed in international and local databases, namely [54], [55], [56] and [57]. They have been cited 9 times, of which 3 are self-citations, 2 are doctoral thesis and 4 are ISI papers.

Two patent applications were submitted within the Electric Machines and Drives Laboratory, namely:

- RO-BOPI 137138 A2 11/2022 (A/00255/14.05.2021): "Five-phase electric motor and method of supplying it with alternating current" ("Motor electric pentafazat și metoda de alimentare a acestuia în curent alternativ")
- RO-BOPI 137140 A2 11/2022 (A/00254/14.05.2021): "Static converter for powering five-phase asynchronous motors and control method for dealing with a fault caused by a phase interruption" ("Convertizor static destinat alimentării motoarelor asincrone pentafazate și metoda de comandă pentru tratarea unui defect cauzat de întreruperea unei faze")

PROSPECTS FOR FUTURE DEVELOPMENT

The physical model of the 5-phase IM represents a proof of concept and the experimental results are a quantitative validation. By improving the 5-phase IM and drive, also the different elements in the test bench, will be obtain a qualitative validation of the multiphase system.

The physical model is equipped with temperature sensors in different parts of the machine. A system for real time data acquisition will be used in future measurements.

The waveforms of the stator currents at load operation of the experimental model will be improved firstly by implementing an improved drive command.

Improving performances one open-phase fault operation point will be achieved by improving the stator winding and the drive control.

REFERENCES

[1] E. Ward și H. Härer, „Preliminary investigation of an invertor-fed 5-phase induction motor," *Proc. IEE,* vol. 116, nr. 6, pp. 980-984, 1969.

[2] E. Levi, R. Bojoi, F. Profumo, H. A. Toliyat și S. Williamson, „Multiphase induction motor drives - a technology status review," *IET Electric Power Applications,* vol. 1, nr. 4, pp. 489-516, 2007.

[3] G. Singh, „Multi-phase induction machine drive research—a survey," *Electric Power Systems Research,* vol. 61, nr. 2, pp. 139-147, 2002, DOI: 10.1016/S0378-7796(02)00007-X.

[4] B. Kundrotas, S. Lisauskas și R. Rinkevicience, „Model of Multiphase Induction Motor," *ELEKTRONIKA IR ELEKTROTECHNIKA,* vol. 111, nr. 5, pp. 111-114, 2011, https://doi.org/10.5755/j01.eee.111.5.369.

[5] C. Hodge, S. Williamson și S. Smith, „Direct Drive Marine Porpulsion Motors," *International Conference on Electrical Machines (ICEM), Munchen, Germany,* p. 087, 2002.

[6] M. Shaikh, I. Atif și M. E. Elmahdi, „Five-phase induction motor drive for weak and remote grid system," *International Journal of Engineering, Science and Technology,* vol. 2, nr. 2, pp. 136-154, 2010.

[7] L. Livadaru, C. Nuţescu, A. Munteanu, A. Simion și M. Cojan, „Comparative FEM-based Analysis of Multiphase Induction Motor," *Analele Universității "Eftimie Murgu" Reșița,* nr. 2, 2014, ISSN 1453 - 7397.

[8] M. I. Masoud, „Five phase induction motor: Phase transposition effect with different stator winding connections," *IEEE,* pp. 1648-1655, 2016, DOI: 10.1109/IECON.2016.7793400.

[9] M. Jones și E. Levi, „A literature survey of state-of-the-art in multi-phase ac drives," *Proc. 36th Univ. Power Eng. Conf. UPEC, Stafford, U.K.,* pp. 587-592, 2002.

[10] C. Kalaivani și K. Rajambal, „Modeling of an efficient high power wind energy conversion system using self-excited multi-phase machines," *Microprocessors and Microsystems,* vol. 74, 2020, https://doi.org/10.1016/j.micpro.2020.103020.

[11] F. Barrero și M. J. Duran, „Recent Advances in the Design, Modeling, and Control of Multiphase Machines—Part I," *IEEE Transactions on Industrial Electronics,* vol. 63, nr. 1, pp. 449-458, 2016, DOI: 10.1109/TIE.2015.2447733.

[12] M. J. Duran și F. Barrero, „Recent Advances in the Design, Modeling, and Control of Multiphase Machines—Part II," *IEEE Transactions on Industrial Electronics,* vol. 63, nr. 1, pp. 459-468, 2016, DOI: 10.1109/TIE.2015.2448211.

[13] G. Renukadevi și K. Rajambal, „Field programmable gate array implementation of space-vector pulse-width modulation technique for Seven-Phase voltage source inverter," *IET Power Electronics,* vol. 7, nr. 2, pp. 376-389, 2014, https://doi.org/10.1049/iet-pel.2013.0078.

[14] G. Renukadevi și K. Rajambal, „Comparison of different PWM schemes for n-phase VSI," IEEE-International Conference On Advances In Engineering," *Science And Management (ICAESM - 2012), Nagapattinam, India,* pp. 559-564, 2012.

[15] K. Chandramohan, S. Padmanaban, R. Kalyanasundaram și F. Blaabjerg, „Modeling of Five-Phase, Self-Excited Induction Generator for Wind Mill Application," *Electric Power Components and Systems, Taylor and Francis,* vol. 46, nr. 3, pp. 353-363, 2018.

[16] E. Levi, S. N. Vukosavic și M. Jones, „Vector control schemes for series-connected six-phase two-motor drive systems," *IEEE Proc. Electr. Power Appl.,* vol. 152, nr. 2, 2005.

[17] G. K. Singh, „A six-phase synchronous generator for stand-alone renewable energy generation: experimental analysis," *Energy,* vol. 36, nr. 3, pp. 1768-1775, 2011, https://doi.org/10.1016/j.energy.2010.12.052.

[18] H. S. Che, E. Levi, M. Jones, M. J. Duran, W.-P. Hew și N. A. Rahim, „Operation of a Six-Phase Induction Machine Using Series-Connected Machine-Side Converters," *IEEE Transactions on Industrial Electronics,* vol. 61, nr. 1, pp. 164-176, 2014, DOI: 10.1109/TIE.2013.2248338.

[19] G. K. Singh, K. B. Yadav și R. P. Saini, „Capacitive self-excitation in six-phase induction generator for small hydro power – an experimental investigation," *International Conference on Power Electronic, Drives and Energy Systems, New Delhi, India,* pp. 1-6, 2006, DOI: 10.1109/PEDES.2006.344267.

[20] G. K. Singh, „Steady-state performance analysis of six-phase self-excited induction generator for renewable energy generation," *International Conference on Electrical Machines and Systems, Wuhan, China,* pp. 2255-2260, 2008.

[21] C. Kalaivani și K. Rajambal, „Dynamic Modeling of Seven-Phase Induction Generator," *Energy Procedia,* vol. 117, pp. 369-376, 2017, https://doi.org/10.1016/j.egypro.2017.05.148.

[22] K. Chandramohan, S. Padmanaban, R. Kalyanasundaram, M. S. Bhaskar și L. Mihet-Popa, „Grid Synchronization of a Seven-Phase Wind Electric Generator Using d-q PLL," *Energies,* vol. 10, p. 926, 2017, https://doi.org/10.3390/en10070926.

[23] D. Casadei, M. Mengoni, G. Serra, A. Tani și L. Zarri, „Comparison of different fault-tolerant control strategies for seven-phase induction motor drives," *13th European Conference on Power Electronics and Applications, Barcelona, Spain,* pp. 1-9, 2009.

[24] Z. Husain, R. K. Singh și S. N. Tiwari, „Multiphase (6-Phase & 12-Phase) Transmission Lines: performance Characterstics," *International Journal of Mathematics and Computers in Simulation,* vol. 1, nr. 2, 2007.

[25] N. E. Hassanain și J. E. Fletcher, „Steady-state performance assessment of three- and Seven-Phase permanent magnet generators connected to a diode bridge rectifier under open-circuit faults," *IET Renewable Power Generation,* vol. 4, nr. 5, p. 420–427, 2010.

[26] L. A. Pereira, G. Nicol, L. F. A. Pereira și M. Perin, „Induction distribution of five-phase induction machines under open-phase fault," *ISA Transactions,* vol. 96, pp. 468-478, 2020, https://doi.org/10.1016/j.isatra.2019.06.001.

[27] L. A. Pereira, L. F. Pereira, S. Haffner și G. Nicol, „Unbalanced operation of five-phase induction machines using steady state symmetrical components - part I: theoretical considerations," *Industrial electronics society, IECON 2015-41st annual conference of the IEEE,* p. 001807–12, 2015, http://dx.doi.org/10.1109/IECON.2015.7392363.

[28] L. A. Pereira, L. F. Pereira, S. Haffner și A. H. Silveira, „Unbalanced operation of five-phase induction machines using steady state symmetrical components - part II: Study of typical cases," *Industrial electronics society, IECON 2015-41st annual conference of the IEEE,* p. 001813–8, 2015, http://dx.doi.org/10.1109/IECON.2015.7392364.

[29] H. A. Toliyat, T. A. Lipo și J. C. White, „Analysis of a concentrated winding induction machine for adjustable speed drive applications. I. Motor analysis," *IEEE Trans. Energy Convers.,* vol. 6, nr. 4, p. 679–683, 1991.

[30] H. A. Toliyat, T. A. Lipo și J. C. White, „Analysis of a concentrated winding induction machine for adjustable speed drive applications. II. Motor design and performance," *IEEE Trans. Energy Convers.,* vol. 6, nr. 4, p. 684–692, 1991.

[31] A. S. Abdel-Khalik și S. Ahmed, „Performance evaluation of a five-phase modular winding induction machine," *IEEE Trans. Ind. Electron.,* vol. 59, nr. 6, p. 2654–2669, 2012.

[32] N. A. Elmalhy, M. M. Ahmed, S. Ahmed și I. ElArabawy, „Performance of a five-phase induction machine with single-tooth winding under open phase conditions," *Proc. 4th Int. Conf. Electric Power Energy Convers. Syst.,* pp. 1-6, 2015.

[33] G. Rezazadeh, S. Vaschetto, F. Tahami, G. A. Capolino, H. Henao și Z. Nasiri-Gheidari, „Analysis of six-phase induction motor with distributed and concentrated windings by using the winding function method," *Proc. XXIII Int. Conf. Elect. Mach.,* p. 2423–2429, 2018.

[34] G. Rezazadeh, F. Tahami, G. A. Capolino, S. Vaschetto, Z. Nasiri-Gheidari și H. Henao, „Improvement of Concentrated Winding Layouts for Six-Phase Squirrel Cage Induction Motors," *IEEE Transactions on Energy Conversion,* vol. 35, nr. 4, pp. 1727-1735, 2020, DOI: 10.1109/TEC.2020.2995433.

[35] S. He, X. Sui, D. Zhou și F. Blaabjerg, „Torque Ripple Minimization of Seven-Phase Induction Motor under More-than-Two-Phase Fault," *2020 International Conference on Electrical Machines (ICEM), Gothenburg,* pp. 2222-2228, 2020.

[36] A. Gonzalez-Prieto, J. J. Aciego, I. Gonzalez-Prieto și M. J. Duran, „Automatic Fault-Tolerant Control of Multiphase Induction Machines: A Game Changer," *Electronics,* vol. 9, p. 938, 2020, https://doi.org/10.3390/electronics9060938.

[37] W. Kong, M. Kang, D. Li, R. Qu, D. Jiang și C. Gan, „Investigation of Spatial Harmonic Magnetic Field Coupling Effect on Torque Ripple for Multiphase Induction Motor Under Open Fault Condition," *IEEE Transactions on Power Electronics,* vol. 33, nr. 7, pp. 6060-6071, 2018, doi: 10.1109/TPEL.2017.2737027.

[38] L. Schreier, J. Bendl și M. Chomat, „Operation of five-phase induction motor after loss of one phase of feeding source," *ElectrEng,* vol. 99, pp. 9-18, 2017.

[39] D. Casadei, M. Mengoni, G. Serra, A. Tani și L. Zarri, „Theoretical and experimental analysis of fault-tolerant control strategies for seven-phase induction motor drives," *SPEEDAM, Pisa,* pp. 1628-1633, 2010.

[40] I. Petrov și J. Pyrhonen, „Performance of Low-Cost Permanent Magnet Material in PM Synchronous Machines," *IEEE Transactions on Industrial Electronics,* vol. 60, nr. 6, pp. 2131-2138, 2013, doi: 10.1109/TIE.2012.2191757.

[41] I. Petrov și J. Pyrhönen, „Performance comparison of an induction machine and line-start PM motor for cooling fan applications," *21st Southern African Universities Power Engineering Conference (SAUPEC),* pp. 122-126, 2013, DOI:10.13140/RG.2.1.2542.1922.

[42] T. Marcic, B. Stumberger și G. Stumberger, „Comparison of Induction Motor and Line-Start IPM Synchronous Motor Performance in a Variable-Speed Drive," *IEEE Transactions on Industry Applications,* vol. 48, nr. 6, pp. 2341-2352, 2012, doi:10.1109/TIA.2012.2227095.

[43] M. Melfi, S. Evon și R. McElveen, „Induction versus permanent magnet motors," *IEEE Industry Applications Magazine,* vol. 15, nr. 6, pp. 28-35, 2009, doi:10.1109/mias.2009.934443.

[44] O. Dobzhanskyi, E. Amiri și R. Gouws, „Comparison analysis of electric motors with two degrees of mechanical freedom: PM synchronous motor vs induction motor," *II International Young Scientists Forum on Applied Physics and Engineering (YSF), Kharkiv, Ukraine,* pp. 14-17, 2016, doi: 10.1109/YSF.2016.7753750.

[45] A. Murray, M. Palma și A. Husain, „Performance Comparison of Permanent Magnet Synchronous Motors and Controlled Induction Motors in Washing Machine Applications Using Sensorless

Field Oriented Control," *IEEE Industry Applications Society Annual Meeting, Edmonton, AB, Canada,* pp. 1-6, 2008, doi: 10.1109/08IAS.2008.11.

[46] V. T. Buyukdegirmenci, A. M. Bazzi și P. T. Krein, „Evaluation of Induction and Permanent-Magnet Synchronous Machines Using Drive-Cycle Energy and Loss Minimization in Traction Applications," *IEEE Transactions on Industry Applications,* vol. 50, nr. 1, pp. 395-403, 2014, doi:10.1109/TIA.2013.2266352.

[47] Z. Yang, F. Shang, I. P. Brown și M. Krishnamurthy, „Comparative Study of Interior Permanent Magnet, Induction, and Switched Reluctance Motor Drives for EV and HEV Applications," *IEEE Transactions on Transportation Electrification,* vol. 1, nr. 3, pp. 245-254, 2015, doi: 10.1109/TTE.2015.2470092.

[48] T. -C. Jeong et al., „Current Harmonics Loss Analysis of 150-kW Traction Interior Permanent Magnet Synchronous Motor Through Co-Analysis of d-q Axis Current Control and Finite Element Method," *IEEE Transactions on Magnetics,* vol. 49, nr. 5, pp. 2343-2346, 2013, doi: 10.1109/TMAG.2013.2246552.

[49] G. Pellegrino, A. Vagati, P. Guglielmi și B. Boazzo, „Performance Comparison Between Surface-Mounted and Interior PM Motor Drives for Electric Vehicle Application," *IEEE Transactions on Industrial Electronics,* vol. 59, nr. 2, pp. 803-811, 2012, doi: 10.1109/TIE.2011.2151825.

[50] G. Volpe, J. Goss, I. Foley, F. Marignetti, M. Popescu și D. A. Staton, „High-Performance Electric Motor for Motor Sport Application," *IEEE Vehicle Power and Propulsion Conference (VPPC), Belfort, France,* pp. 1-5, 2017, doi: 10.1109/VPPC.2017.8330886.

[51] J. Kim, D. Kang, T. Jeong, D. Jeong, J. Lee și S. Lee, „Optimal Rotor Design of an 150 kW-Class IPMSM by the 3-D Voltage–Inductance-Map Analysis Method," *IEEE Transactions on Magnetics,* vol. 53, nr. 11, pp. 1-5, 2017, doi: 10.1109/TMAG.2017.2707391.

[52] Y. Yang et al., „Design and Comparison of Interior Permanent Magnet Motor Topologies for Traction Applications," *IEEE Transactions on Transportation Electrification,* vol. 3, nr. 1, pp. 86-97, 2017, doi: 10.1109/TTE.2016.2614972.

[53] G. Pellegrino, A. Vagati, B. Boazzo și P. Guglielmi, „Comparison of Induction and PM Synchronous Motor Drives for EV Application Including Design Examples," *IEEE Transactions on Industry Applications,* vol. 48, nr. 6, pp. 2322-2332, 2012, doi: 10.1109/TIA.2012.2227092.

[54] V. Fireţeanu, A. -I. Constantin și C. Dumitru, „Finite Element Analysis of the Tolerance of the Multi-Phase Induction Motors regarding Stator Winding Failures," *IEEE Workshop on Electrical Machines Design, Control and Diagnosis (WEMDCD), Modena, Italy,* pp. 266-271, 2021, doi: 10.1109/WEMDCD51469.2021.9425668.

[55] V. Fireţeanu, A. -I. Constantin și C. Dumitru, „Finite Element Analysis of the Performances of the 3-Phase, 5-Phase, 7-Phase and 9-Phase Squirrel-Cage Induction Motors," *12th International Symposium on Advanced Topics in Electrical Engineering (ATEE), Bucharest, Romania,* pp. 1-6, 2021, doi: 10.1109/ATEE52255.2021.9425068.

[56] V. Fireţeanu și C. Dumitru, „Finite Element Analysis of Multiphase Permanent Magnet Synchronous Motors with the Same Stators of Analogue 3-phase, 5-phase, 7-phase and 9-phase Induction Motors," *2021 International Conference on Applied and Theoretical Electricity (ICATE), Craiova, Romania,* pp. 1-6, 2021, doi: 10.1109/ICATE49685.2021.9465021.

[57] C. Dumitru, „A case study for a five phase induction motor using Finite Element Analysis on healthy operation and operation with an open-phase fault," *13th International Symposium on Advanced Topics in Electrical Engineering (ATEE), Bucharest, Romania,* pp. 1-6, 2023, doi: 10.1109/ATEE58038.2023.10108326.

[58] I. Cioc și C. Nica, Proiectarea mașinilor electrice, București: Editura Didactică și Pedagogică, R.A. - București, 1994.

[59] Îndrumător de proiectare a mașinii asincrone, Universitatea Tehnică din Cluj-Napoca, Catedra de Mașini electrice, 2002.

[60] J. Pyrhönen, T. Jokinen și V. Hrabovcova, Design of Rotating Electrical Machines, First Edition, John Wiley & Sons, Ltd. ISBN: 978-0-470-69516-6, 2008.

[61] P. Lombard și F. Zidat, „Determining end ring resistance and inductance of squirrel cage for induction motor with 2D and 3D computations," *XXII International Conference on Electrical Machines (ICEM),* pp. 266-271, 2016, doi: 10.1109/ICELMACH.2016.7732537.

[62] „Altair Engineering Flux2D 2020 Software Documentation".

[63] V. Fireteanu, Analiza în element finit în studiul mașinilor electrice, Editura PRINTECH, 2010, pp 159.

[64] T. Hussain, S. K. Moin Ahmed, A. Iqbal și M. R. Khan, „Five-phase induction motor behaviour under faulted conditions," *Annual IEEE India Conference, Kanpur, India,* pp. 509-513, 2008, doi: 10.1109/INDCON.2008.4768776.